Redox Biology 12 (2017) 438–455

Contents lists available at ScienceDirect

Redox Biology

journal homepage: www.elsevier.com/locate/redox

Research Paper

Resolvin D1 via prevention of ROS-mediated SHP2 inactivation protects endothelial adherens junction integrity and barrier function

Rima Chattopadhyay, Somasundaram Raghavan, Gadiparthi N. Rao*

Department of Physiology, University of Tennessee Health Science Center, Memphis, TN 38163, USA

ARTICLE INFO

Keywords:
Resolvin D1
Endothelial barrier function
Adherens junctions
ROS
SHP2
Inflammation

ABSTRACT

Resolvins are a novel class of lipid mediators that play an important role in the resolution of inflammation, although the underlying mechanisms are not very clear. To explore the anti-inflammatory mechanisms of resolvins, we have studied the effects of resolvin D1 (RvD1) on lipopolysaccharide (LPS)-induced endothelial barrier disruption as it is linked to propagation of inflammation. We found that LPS induces endothelial cell (EC) barrier disruption via xanthine oxidase (XO)-mediated reactive oxygen species (ROS) production, protein tyrosine phosphatase SHP2 inactivation and Fyn-related kinase (Frk) activation leading to tyrosine phosphorylation of α-catenin and VE-cadherin and their dissociation from each other affecting adherens junction (AJ) integrity and thereby increasing endothelial barrier permeability. RvD1 attenuated LPS-induced AJ disassembly and endothelial barrier permeability by arresting tyrosine phosphorylation of α-catenin and VE-cadherin and their dislocation from AJ via blockade of XO-mediated ROS production and thereby suppression of SHP2 inhibition and Frk activation. We have also found that the protective effects of RvD1 on EC barrier function involve ALX/FPR2 and GPR32 as inhibition or neutralization of these receptors negates its protective effects. LPS also increased XO activity, SHP2 cysteine oxidation and its inactivation, Frk activation, α-catenin and VE-cadherin tyrosine phosphorylation and their dissociation from each other leading to AJ disruption with increased vascular permeability in mice arteries and RvD1 blocked all these effects. Thus, RvD1 protects endothelial AJ and its barrier function from disruption by inflammatory mediators such as LPS via a mechanism involving the suppression of XO-mediated ROS production and blocking SHP2 inactivation.

1. Introduction

Many inflammatory diseases arise due to uncontrolled inflammatory response or in other words failure of resolution process [1,2]. Resolution of inflammation is now considered as an actively regulated phenomenon and understanding the signaling events that regulate the termination of inflammation is crucial in the circumvention of inflammatory diseases [1,3]. In recent years, endogenously derived lipid mediators like resolvins, protectins, maresins and lipoxins received special attention due to their anti-inflammatory properties [4–6]. These lipid mediators appear to limit excessive inflammation without any adverse effects on normal immune responses [6,7]. Resolvin D1 (RvD1) is synthesized from docosahexanoic acid (DHA) by sequential oxygenation by enzymes 15-lipoxygenase (15-LOX) and 5-LOX [5,8] and it exhibits potent anti-inflammatory effects both in vitro and in vivo [9]. It was demonstrated that RvD1 reduces ROS production, inflammatory cytokines and adhesion molecules expression and attenuates neutrophil trafficking [5,9,10]. In addition, it has been reported that RvD1 protects endothelial barrier function, although the underlying mechanisms were not well understood [11,12]. The endothelium, which acts as anti-platelet adhesion and anti-thrombotic surface for the circulating blood and with its selective barrier permeability, plays an important role in the maintenance of vascular integrity [13,14]. Disruption of endothelial barrier function facilitates passage of inflammatory cells into the tissues where these cells via expression of various proinflammatory molecules amplify the local and systemic inflammation [15,16].

Adherens junctions (AJ), gap junctions (GJ) and tight junctions (TJ) are important endothelial cell-to-cell adhesions and play an essential role in its barrier function [17,18]. Disruption of these

Abbreviations: AJ, adherens junctions; CD, chow diet; CSN, cysteine sulfonate; DHA, docosahexanoic acid; EV, Evans blue; Frk, Fyn-related kinase; GJ, gap junctions; HUVEC, human umbilical vein endothelial cells; 15-LOX, 15-lipoxygenase; LSGS, low-serum growth supplements; PTK, protein tyrosine kinase; PTP, protein tyrosine phosphatase; RvD1, Resolvin D1; ROS, reactive oxygen species; TER, transendothelial electrical resistance; TJ, tight junctions; VE-cadherin, vascular endothelial cadherin; WB, Western blotting; IP, immunoprecipitation; WT, wild type; XO, xanthine oxidase

* Correspondence to: Department of Physiology, University of Tennessee HSC, 71 S. Manassas Street, Memphis, TN 38163, USA.
E-mail address: rgadipar@uthsc.edu (G.N. Rao).

http://dx.doi.org/10.1016/j.redox.2017.02.023
Received 25 January 2017; Accepted 27 February 2017
Available online 06 March 2017

junctions leads to development of gaps in the endothelial layer, which results in its increased permeability and altered function, a hallmark of various vascular diseases [19–22]. Among the cell-to-cell junctions, AJ are comprised of vascular endothelial (VE) cadherin and its binding partners catenins (α, β, γ and p120) [13]. Impaired expression of AJ proteins affects vascular morphogenesis during embryonic development and vascular permeability in the adulthood [23,24]. In response to inflammatory mediators VE-cadherin gets phosphorylated and either internalizes or degrades leading to loss of endothelial AJ integrity and barrier function [25–27]. Interestingly, both protein kinases (PKs) and protein phosphatases (PPs) have been found to be localized at the AJ, suggesting a role for phosphorylation and dephosphorylation of AJ proteins in the regulation of the maintenance of AJ integrity [19,25,28,29]. In fact, LPS via oxidant-mediated inhibition of PPs has been shown to activate PKs in the modulation of inflammation [30,31]. LPS has also been reported to disrupt endothelial barrier function in the propagation of inflammation [11,12,31,32]. Previously we have reported that arachidonic acid metabolite, 15(S)-HETE, by XO-mediated ROS production leads to activation of Src and Pyk2 in the tyrosine phosphorylation of TJ proteins affecting endothelial TJ integrity and its barrier function [33]. Based on these findings, we asked the question whether RvD1 via inhibiting XO-mediated ROS production and preventing protein tyrosine phosphatases (PTPs) inactivation and protein tyrosine kinases (PTKs) activation protects endothelial barrier function from disruption by LPS. We found that RvD1 by inhibition of LPS-induced XO-mediated ROS production, and preventing SHP2 inactivation and Frk activation, thereby reducing α-catenin and VE-cadherin tyrosine phosphorylation and their dissociation from each other protects endothelial AJ integrity and its barrier function. RvD1 exerts its protective effects on the maintenance of endothelial AJ integrity and its barrier function via activation of its receptors ALX/FPR2 and GPR32. Consistent with these observations, RvD1 also protected endothelial AJ integrity and its barrier function from LPS-induced disruption in mice arteries in vivo as well.

2. Materials and methods

2.1. Reagents

Resolvin D1 (10012554) was purchased from Cayman Chemical Company (Ann Arbor, MI). Fluorescein isothiocyanate-dextran (FD70S), LPS (L4391), PHPS1 (P0039) and xanthine oxidase kit (MAKO78-1KT) were bought from Sigma Aldrich Company (St. Louis, MO). Anti-α-catenin (SC-7894 and SC-9988), anti-β-catenin (SC-7963), anti VE-cadherin (SC-28644 and SC-9989), anti-p120 catenin (SC-23872), anti-α-tubulin (SC-23948), anti-cMyc (SC-789), anti-pLck (SC-101728), anti-Lck (SC-433), anti-pYes (SC-130182), anti-Yes (SC-8403), anti-Fyn (SC-365913), anti-Lyn (SC-15), anti-Frk (SC-166478) and anti-PTPμ (SC-56957) antibodies were procured from Santa Cruz Biotechnology Inc., (Santa Cruz, CA). Anti-pSrc (2101 S) antibody was obtained from Cell Signaling Technology (Beverly, MA). Anti-pFyn (ab192172) and anti-VE-cadherin (ab33168) antibodies were bought from Abcam (Cambridge, MA). Anti-PY20 (05–777), anti-Src (05–184), anti-pLyn (04–375), anti-PTP-PEST (05–1417) and anti-FPR2 (ABF118) antibodies and PTP assay kit (17–125) were obtained from Millipore (Temecula, CA). Anit-SHP2 (610622) and anti-SHP1 (610126) antibodies were purchased from BD Biosciences (San Jose, CA). Anti-cysteine sulfonate antibody (ADI-OSA-820-F) was bought from Enzo Life Sciences (Farmingdale, NY). Wild type SHP2 (12283) and mutant SHP2 (C459S) (12284) plasmids were received from Addgene (Cambridge, MA) [34]. Anti-GPR32 neutralizing antibody (GTX71225) was obtained from Genetex (Irvine, CA). BOC2 (07201) was purchased from Phoenix Pharmaceuticals (Burlingame, CA). Hoechst 33342 (10 mg/ml) solution (H3570), goat anti-rabbit, and goat anti-mouse secondary antibodies conjugated with Alexa Fluor 568 (A11011) or Alexa Fluor 488 (A11029) fluorochrome, ProLong Gold antifade reagent (P36930), Medium 200 (M200500), low serum growth supplements (S003K), Lipofectamine 3000 (L3000015), non-targeting siRNA (D-001810-10), Frk siRNA (S5363), and gentamycin/amphotericin solution (R01510) were bought from ThermoFisher Scientific (Carlsbad, CA). The enhanced chemiluminescence (ECL) Western blotting detection reagents (RPN2106) were obtained from GE Healthcare (Pittsburg, PA).

2.2. Animals

C57BL/6 mice were purchased from Charles River Laboratories (Wilmington, MA). Mice were maintained at UTHSC vivarium according to the Institutional Animal Care and Use Committee's guidelines. The experiments involving animals were approved by the Animal Care and Use Committee of the University of Tennessee Health Science Center, Memphis, TN. To study the effect of RvD1 on the protection of endothelial barrier function, mice were kept on chow diet (CD) and administered intraperitoneally with RvD1 at a dose of 10 μg/kg body weight [35] every third day for a total of one week before the administration of (5 mg/kg body weight) LPS [36]. Twenty-four hrs after the administration of LPS, the mice were sacrificed, aortas were isolated and used as required.

2.3. Cell culture

Human umbilical vein endothelial cells (HUVECs) were purchased from Invitrogen (C0035C) and cultured in Medium 200 containing low serum growth supplements (LSGS), 10 μg/ml gentamycin and 0.25 μg/ml amphotericin B. Cultures were maintained at 37 °C in a humidified 95% air and 5% CO_2 atmosphere. HUVECs between 6 and 10 passages were growth-arrested by incubating in Medium 200 without LSGS for 12 h and used to perform the experiments unless otherwise indicated.

2.4. Transfections

HUVECs were transfected with the indicated siRNA at a final concentration of 100 nM using Lipofectamine 3000 transfection reagent according to the manufacturer's instructions. After transfections, cells were quiesced in Medium 200 without LSGS for 12 h and used as required.

2.5. Western blot analysis

Cell or tissue extracts containing an equal amount of protein from control and the indicated treatments were resolved by SDS-PAGE. The proteins were transferred electrophoretically to a nitrocellulose membrane. After blocking in either 5% (W/V) nonfat dry milk or 5% (W/V) BSA, the membrane was probed with appropriate primary antibodies followed by incubation with horseradish peroxidase-conjugated secondary antibodies. The antigen-antibody complexes were detected using enhanced chemiluminescence detection reagents as described previously [33].

2.6. Immunoprecipitation

Immunoprecipitation was performed as described by us previously [33]. Cell or tissue extracts containing an equal amount of protein from control and each treatment was incubated with the indicated primary antibody at 1:100 dilution overnight at 4 °C. Protein A/G-conjugated Sepharose CL-4B beads were added and incubation continued for an additional 1 h at room temperature and the beads were collected by centrifugation at 1000 rpm for 1 min at 4 °C. The beads were washed three times with lysis buffer and once with PBS, boiled in SDS sample buffer and analyzed by immunoblotting.

2.7. Immunofluorescence

HUVECs were grown to a confluent monolayer on cell culture grade glass cover slips, quiesced and treated with and without LPS (500 ng/ml) [37] in the presence and absence of RvD1 (200 ng/ml) [12] alone or in combination with the indicated inhibitors for the indicated time periods. After the treatments, cells were washed with cold PBS, fixed with 95% ethanol for 30 min at 4 °C, permeabilized in TBS (10 mM Tris-HCl, pH 8.0, 150 mM NaCl) containing 0.1% Triton X-100 for 10 min at room temperature and blocked with 2% BSA in TBS containing 10 mM $CaCl_2$, 5 mM $MgCl_2$ and 0.1% saponin overnight at 4 °C. After incubation with appropriate primary antibodies (1:200 dilution), Alexa Flour-conjugated secondary antibodies were added (1:500 dilution) and incubation continued for 1 h at room temperature, counter stained with Hoechst 33342 (1:3000 dilution in PBS) for 2 min at room temperature and mounted onto glass slides with Prolong Gold antifade mounting medium. In the case of aortas, after dissection they were cleaned from fat tissue, opened longitudinally, fixed with 2% paraformaldehyde for 1 h, permeabilized with 0.2% Triton-X-100 in PBS for 20 min and blocked in PBS containing 0.1% Triton-X-100% and 5% FBS for 1 h at room temperature before being incubated with primary and secondary antibodies. Fluorescence images of the cells and aortas were captured using an inverted Zeiss fluorescence microscope (AxioObserver Z1) via a 40X (NA 0.6) objective and AxioCam MRm camera without any enhancements using the microscope operating and image analysis software AxioVision Version 4.7.2 (Carl Zeiss Imaging Solutions GmbH).

2.8. Flux assay

HUVECs were grown to a confluent monolayer on the apical side of a polycarbonate membrane of a transwell (0.4 μm pore size) and growth-arrested for 6 h. The monolayer was treated with and without LPS (500 ng/ml) in the presence and absence of RvD1 (200 ng/ml) for 2 h. FITC-conjugated dextran (MW ~70 kDa) was added to the basal chamber at 100 μg/ml concentration along with LPS and after 2 h the fluorescence intensity of the medium from each chamber was measured using SpectraMax Gemini XS spectrofluorometer (Molecular Devices). Whenever siRNA was used, HUVECs were transfected first with the siRNA and then seeded onto the transwell and in the case of pharmacological inhibitors or neutralizing antibodies, they were added 30 min prior to the addition of RvD1 and/or LPS. The flux was expressed as % dextran diffused/h/cm^2 as described previously [33].

2.9. Transendothelial electrical resistance (TER)

HUVECs were grown to a confluent monolayer on the apical side of a polycarbonate membrane of a transwell (0.4 μm pore size) and growth-arrested for 6 h. The growth-arrested EC monolayer was treated with and without LPS (500 ng/ml) in the presence and absence of RvD1 (200 ng/ml) alone or in combination with the indicated inhibitors or neutralizing antibodies for the indicated time periods. Whenever siRNA was used, HUVECs were transfected first with the siRNA and then seeded onto the transwell and in the case of pharmacological inhibitors or neutralizing antibodies, they were added 30 min prior to the addition of RvD1 and/or LPS. TER was measured at various time points using a Millicell ERS-2 V-Ohm Meter (MERS00002, EMD Millipore) and expressed as Ω cm^2 [38].

2.10. ROS production

Intracellular ROS production was determined as described previously [33]. After the treatments, HUVECs were incubated with 10 mM CM-H2DCFDA for 30 min, washed with PBS, suspended in serum-free medium and the fluorescence intensities were measured in a SpectraMax Gemini XS spectrofluorometer (Molecular Devices) with excitation at 485 nm and emission at 535 nm. The ROS production was expressed as RFU.

2.11. XO activity

Xanthine oxidase activity was measured using a kit according to the manufacturer's instructions.

2.12. PTP assay

PTP activity was measured by dephosphorylation of PTP-specific phosphopeptide and the inorganic phosphate released was detected by malachite green reagent kit. To measure SHP2 activity, the cell extracts containing equal amounts of protein were immunoprecipitated with anti-SHP2 antibodies and the immunocomplexes were assayed for PTP activity as described Ram and Waxman [39].

2.13. Miles assay

Vascular permeability was measured by Miles assay [40]. Mice fed with CD were administered with RvD1 at a dose of 10 μg/kg body weight every third day for a total of one week followed by injection of LPS (5 mg/kg body weight). After 24 h, mice were anesthetized and 0.1 ml of 1% Evans blue dye was injected into the tail vein. After 20 min, blood vessels were perfused with PBS through the left ventriculum and aortas were isolated. After taking photographs, Evans blue dye was extracted from the arteries by incubating in formaldehyde at 55 °C for 24 h and the optical density was measured at 610 nm. Vascular permeability was expressed as the amount of Evans blue dye extravasated per mg artery.

2.14. Statistics

All the experiments were performed three times and the data were presented as Mean ± SD. The treatment effects were analyzed by one-way ANOVA followed by Student *t*-test and the p values < 0.05 were considered to be statistically significant.

3. Results

3.1. RvD1 blocks LPS-induced AJ protein tyrosine phosphorylation, AJ disruption and endothelial barrier dysfunction

RvD1 has been reported to reduce inflammation but the underlying mechanisms were not well understood. Since endothelial barrier permeability plays an important role in the propagation of inflammation, we asked the question whether RvD1 has any role in the regulation of endothelial barrier integrity, thereby in the maintenance of tissue homeostasis [13,19]. To address this question, we first tested the effect of RvD1 on endothelial barrier function. LPS, a potent inflammatory molecule, disrupted endothelial barrier function as measured by increased dextran flux and decreased transendothelial electrical resistance (TER) and RvD1 prevented these effects (Fig. 1A & B). To understand the mechanisms, we tested the effect of LPS on the integrity of AJs, which plays an important role in the maintenance of endothelial barrier function [19]. As shown in Fig. 1C, LPS did not affect the steady state levels of AJ proteins, namely VE-cadherin, α-catenin, β-catenin and p120-catenin. Previously, we have reported that threonine/tyrosine phosphorylation of TJ proteins is involved in a 15-LOX metabolite of AA, 15(S)-HETE-induced TJ disruption and endothelial barrier dysfunction [33,41]. Based on these observations, in the present study we tested whether LPS induces AJ protein tyrosine phosphorylation leading to their disruption and RvD1 was able to alleviate these effects. Towards this end, we first studied a time course effect of LPS

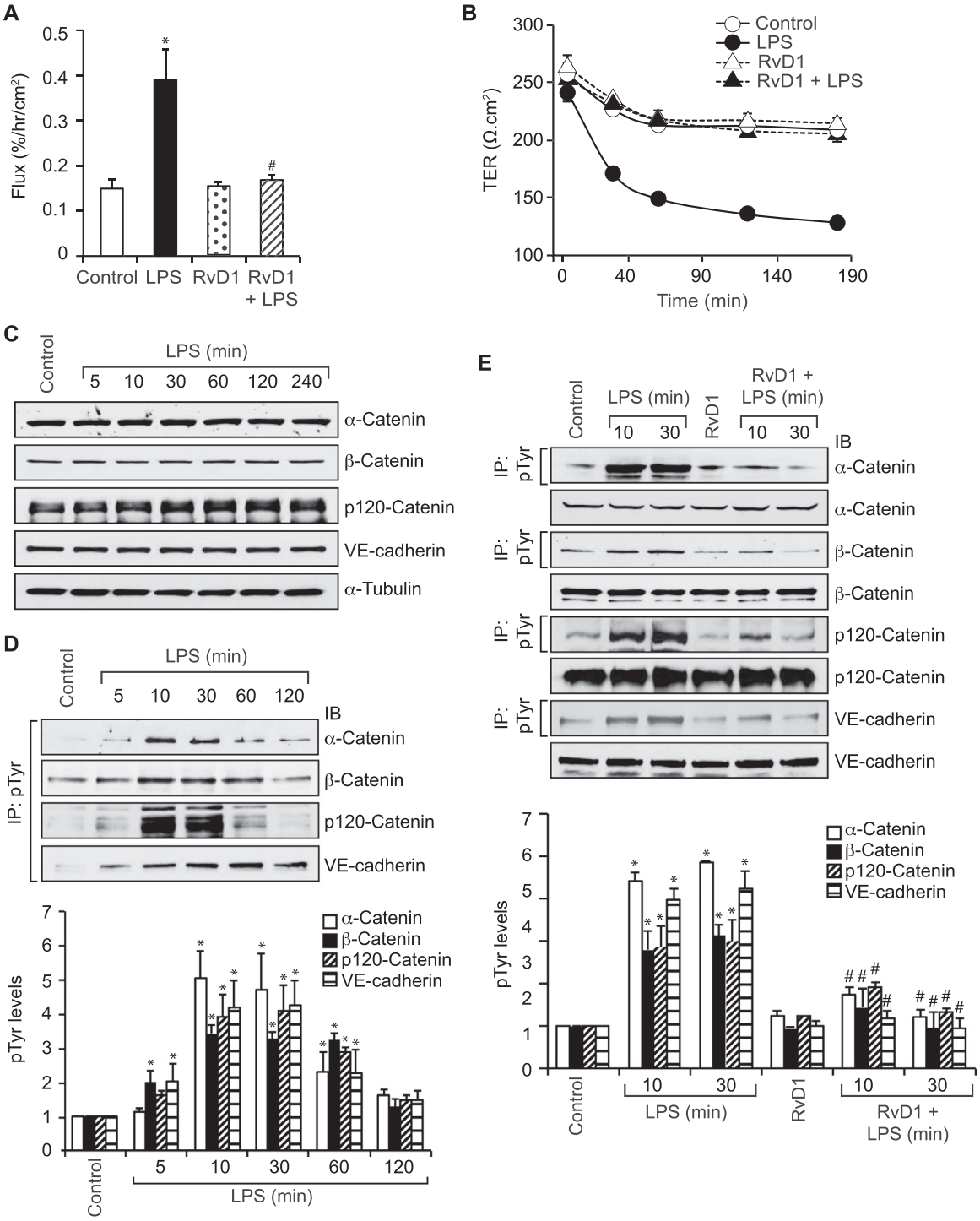

Fig. 1. RvD1 attenuates LPS-induced endothelial barrier permeability via blockade of AJ protein tyrosine phosphorylation. A & B. Quiescent HUVEC monolayer was treated with and without LPS (500 ng/ml) in the presence and absence of RvD1 (200 ng/ml) for 2 h or the indicated time periods and dextran flux (~75 kDa) (A) and TER (B) were measured, respectively. C & D. Quiescent HUVECs were treated with and without LPS (500 ng/ml) for the indicated time periods, cell extracts were prepared and equal amounts of proteins from control and each treatment were either analyzed by Western blotting (WB) for the steady state levels of the indicated proteins (C) or immunoprecipitated with pTyr antibodies and the immunocomplexes were analyzed by immunoblotting (IB) for the indicated proteins (D) using their specific antibodies. E. Quiescent HUVECs were treated with and without LPS (500 ng/ml) in the presence and absence of RvD1 (200 ng/ml) for the indicated time periods, cell extracts were prepared and equal amounts of proteins from control and each treatment were immunoprecipitated with pTyr antibodies and the immunocomplexes were analyzed by IB for the indicated proteins. The same cell extracts were also analyzed by WB for the indicated protein total levels. The bar graphs represent quantitative analysis of three experiments. The values are expressed as Means ± SD. *, $p < 0.05$ vs control; #, $p < 0.05$ vs LPS.

on tyrosine phosphorylation of AJ proteins. LPS induced the tyrosine phosphorylation of AJ proteins, particularly α-catenin and VE-cadherin more robustly (Fig. 1D). In addition, RvD1 inhibited the LPS-induced tyrosine phosphorylation of these proteins (Fig. 1E). Next, we performed co-immunoprecipitation (Co-IP) experiment to find whether tyrosine phosphorylation of α-catenin and VE-cadherin leads to their dissociation from AJ. Co-IP experiment showed that VE-cadherin exists in complex with all three catenins in a quiescent HUVEC monolayer and in response to LPS only α-catenin but not β-catenin or p120-catenin dissociates from

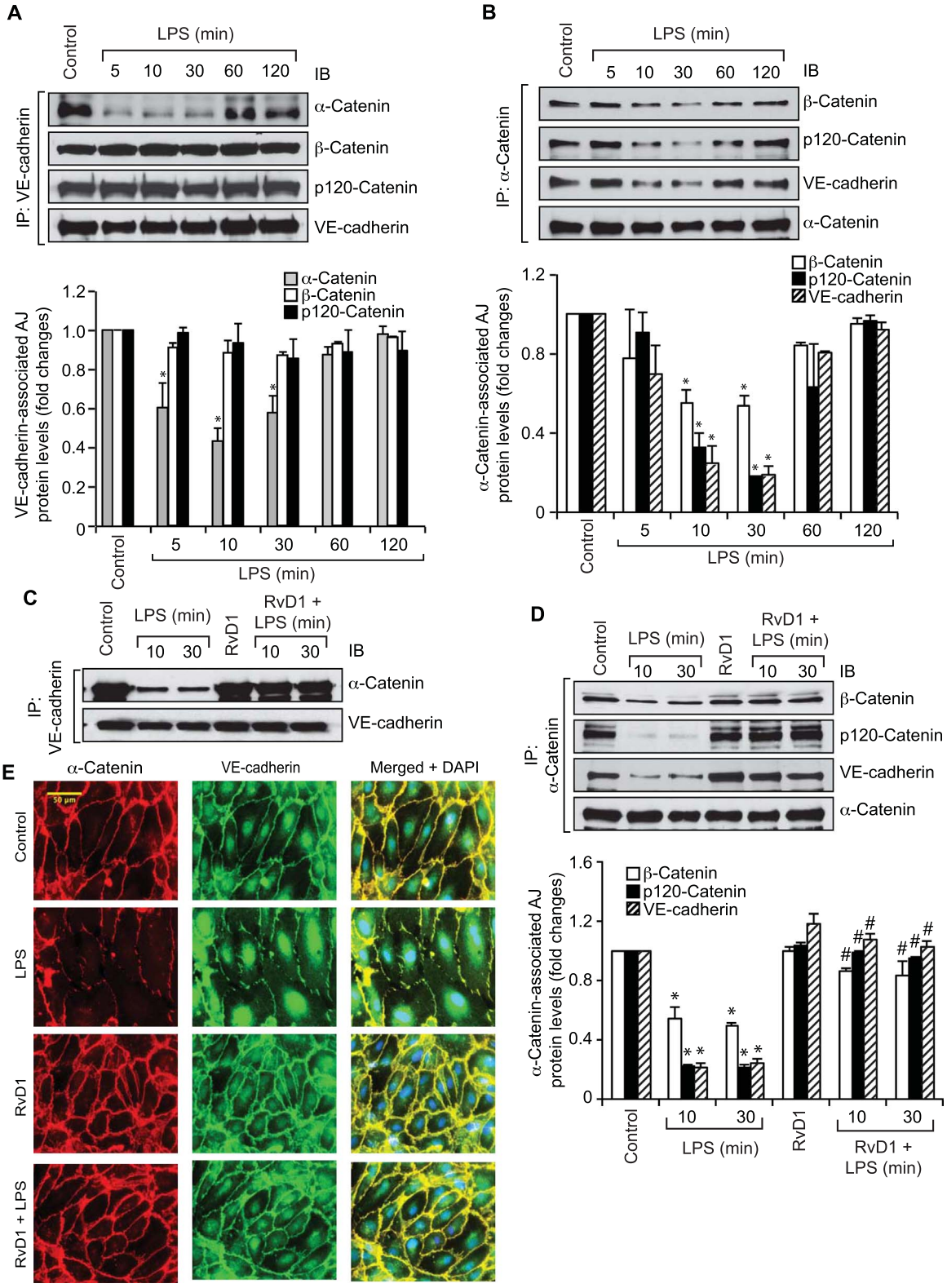

Fig. 2. RvD1 blocks LPS-induced AJ disruption. A & B. Quiescent HUVECs were treated with and without LPS (500 ng/ml) for the indicated time periods, cell extracts were prepared and equal amounts of proteins from control and each treatment were immunoprecipitated with VE-cadherin or α-catenin antibodies and the immunocomplexes were analyzed by IB for the indicated proteins using their specific antibodies. C & D. Quiescent HUVECs were treated with and without LPS (500 ng/ml) in the presence and absence of RvD1 (200 ng/ml) for the indicated time periods, cell extracts were prepared and equal amounts of proteins from control and each treatment were immunoprecipitated with VE-cadherin or α-catenin antibodies and the immunocomplexes were analyzed by IB for the indicated proteins. E. Quiescent HUVEC monolayer was treated with and without LPS (500 ng/ml) in the presence and absence of RvD1 (200 ng/ml) for 30 min, fixed and stained double immunofluorescently for α-catenin and VE-cadherin using mouse anti-α-catenin and rabbit anti-VE-cadherin antibodies followed by developing with Alexa Fluor 568-conjugated goat anti-mouse and Alexa Fluor 488-conjugated goat anti-rabbit secondary antibodies, respectively. The images were captured using an inverted Zeiss fluorescence microscope (AxioObserver Z1) via a 40X (NA 0.6) objective and AxioCam MRm camera without any enhancements. The bar graphs in panels A, B and D represent Mean ± SD values of three experiments, *, $p < 0.05$ vs control; #, $p < 0.05$ vs LPS.

VE-cadherin (Fig. 2A). In a converse experiment, we found both β-catenin and p120-catenin as well as VE-cadherin dissociate from α-catenin in response to LPS (Fig. 2B). These results infer that α-catenin, β-catenin and p120-catenin bind to VE-cadherin and in response to LPS only α-catenin but not β-catenin or p120-catenin dissociate from it. Based on these results, we examined whether RvD1 was able to prevent the dissociation of α-catenin from VE-cadherin. Indeed, LPS induced dissociation of α-catenin from VE-cadherin and RvD1 prevented their dissociation (Fig. 2C & D). To confirm these observations, we performed co-immunofluorescence staining for α-catenin and VE-cadherin complex in AJ. Co-immunofluorescence staining showed that α-catenin co-localizes with VE-cadherin in AJ of HUVEC monolayer and upon treatment with LPS they appear to be dissociated from each other and from AJ and RvD1 was able to suppress these effects (Fig. 2E).

3.2. RvD1 suppresses Frk activation in the blockade of LPS-induced AJ protein tyrosine phosphorylation, AJ disruption and endothelial barrier dysfunction

To identify the tyrosine kinase(s) that mediates LPS-induced AJ protein tyrosine phosphorylation and their disruption, we tested the role of the Src family of PTKs using a pharmacological approach. PP1 and PP2, two potent inhibitors of the Src family of PTKs [33], blocked LPS-induced tyrosine phosphorylation of α-catenin and VE-cadherin as well as their dissociation from each other (Fig. 3A). This result suggests a role for the Src family of PTKs in the tyrosine phosphorylation of α-catenin and VE-cadherin and their dissociation from each other. To identify the Src family of PTKs activated by LPS, we performed a time course effect. LPS stimulated tyrosine phosphorylation of several members of the Src family of PTKs, including Frk, Fyn, Lyn and Yes and RvD1 suppressed this effect (Fig. 3B & C). Since RvD1 blocked LPS-induced Frk phosphorylation completely, we further tested the role of this kinase in LPS-induced α-catenin and VE-cadherin tyrosine phosphorylation and their dissociation from each other. Downregulation of Frk levels by siRNA approach attenuated both α-catenin and VE-cadherin tyrosine phosphorylation and their dissociation from each other (Fig. 3D). Frk downregulation also prevented their dissociation from AJ as measured by co-immunofluorescence staining (Fig. 3E). In addition, depletion of Frk levels blocked LPS-induced increase in endothelial barrier permeability and reversed the decrease in its TER (Fig. 3F & G).

3.3. RvD1 inhibits XO-mediated ROS production in the blockade of LPS-induced Frk activation, AJ protein tyrosine phosphorylation, AJ disruption and endothelial barrier dysfunction

Many reports have shown a link between XO-mediated ROS production and endothelial dysfunction [42–44]. Previously, we have shown that XO via ROS production was involved in the activation of Src and Pyk2 in 15(S)-HETE-induced endothelial TJ protein tyrosine phosphorylation, TJ disruption and its barrier dysfunction [33]. Therefore, to understand the mechanisms by which RvD1 prevents Frk-mediated tyrosine phosphorylation of α-catenin and VE-cadherin, we have studied the effect of RvD1 on LPS-induced XO activity. LPS induced both ROS production and XO activity in a time dependent manner and RvD1 suppressed these effects (Fig. 4A & B). To find whether LPS-induced ROS production was dependent on XO activity, we tested the effect of Allopurinol, a specific inhibitor of XO [43]. Allopurinol completely blocked LPS-induced ROS production (Fig. 4C). This result infers that XO mediates LPS-induced ROS production. In lieu of these observations, we further tested the role of XO in LPS-induced Frk activation, α-catenin and VE-cadherin tyrosine phosphorylation and their disruption from AJ. Allopurinol inhibited LPS-induced Frk activation, α-catenin and VE-cadherin tyrosine phosphorylation and their dissociation from each other as well as from AJ (Fig. 4D & E). Consistent with these observations, Allopurinol also blocked LPS-induced endothelial dextran flux and reversed the decrease in its TER (Fig. 4F & G).

3.4. Suppression of SHP2 inactivation is required for RvD1 in the blockade of LPS-induced Frk activation, AJ protein tyrosine phosphorylation, AJ disruption and EC barrier dysfunction

It is known that PTPs play a role in regulation of endothelial barrier permeability [18,19,25,28,31]. In addition, ROS via oxidation of catalytic cysteine residues inactivates the PTPs [19,25,31]. Since we found that RvD1 suppresses LPS-induced ROS production, it might be possible that RvD1 via its capacity to suppress ROS production might be preventing the inactivation of a PTP. To address this assumption, we tested the effect of RvD1 on PTP activity. LPS decreased the PTP activity and RvD1 prevented this effect (Fig. 5A). To identify the PTP inactivated by LPS we first examined for PTPs associated with AJ. The co-IP experiment showed that several PTPs including PTP-PEST, PTPμ, SHP1 and SHP2 exist in complex with VE-cadherin and in response to LPS, SHP2 dissociates from VE-cadherin and RvD1 prevents this effect (Fig. 5B). In a converse experiment, we also found that both α-catenin and VE-cadherin dissociate from SHP2 in RvD1-sensitive manner (Fig. 5C). Furthermore, LPS inhibited SHP2 activity and RvD1 prevented this effect (Fig. 5D). Consistent with the assumption that ROS inhibit PTP activity, Allopurinol that blocked LPS-induced ROS production also prevented LPS-induced SHP2 inactivation (Fig. 5E). Thus, it appears that LPS inactivates the PTP, SHP2, by XO-mediated ROS production and RvD1 by suppressing XO-mediated ROS production prevents its inactivation. LPS causes inactivation of SHP2 by oxidation of its cysteine residue at 459 [45]. To understand the mechanism of RvD1-mediated rescue of SHP2 activity from inhibition by LPS, we tested the effect of RvD1 on LPS-induced cysteine oxidation of SHP2. We found that LPS induces SHP2 cysteine oxidation and RvD1 prevents this effect (Fig. 5F). Allopurinol also prevented the LPS-induced SHP2 cysteine oxidation (Fig. 5G). To confirm these findings, we next used expression vectors for WT and a phosphatase-dead cysteine (C459S) mutant SHP2 [45]. Cells were transfected with WT or C459S mutant SHP2, quiesced, treated with and without LPS (500 ng/ml) in the presence and absence of RvD1 (200 ng/ml) for 30 min and examined for SHP2 cysteine oxidation and its activity. In response to LPS, WT SHP2 showed increased cysteine oxidation and decreased activity and RvD1 prevented these effects (Fig. 5H & I). In contrast, in the case of C459S mutant SHP2, LPS failed to cause its cysteine oxidation and no obvious differences were noted in its activity between control and the indicated treatments, as it was a phosphatase-dead mutant (Fig. 5H & I). These observations suggest that RvD1 prevents SHP2 inactivation by blocking its cysteine oxidation. To confirm the protective role of SHP2 against LPS-induced endothelial AJ disruption and its barrier dysfunction we used a pharmacological approach. In the presence of SHP2 inhibitor, PHPS1 [46], RvD1 failed to prevent the effects of LPS on Frk activation, α-catenin and VE-cadherin tyrosine phosphorylation and their dissociation from each other as well as from AJ (Fig. 6A & B). Similarly, in the presence of SHP2 inhibitor, RvD1 also failed to prevent LPS-induced increase in endothelial dextran flux and to reverse the decrease in its TER (Fig. 6C & D). These observations demonstrate that prevention of SHP2 inactivation is required for RvD1-mediated protection of endothelial AJ integrity and its barrier function.

3.5. Both ALX/FPR2 and GPR32 mediate the protective effects of RvD1 against LPS-induced endothelial AJ disruption and its barrier dysfunction

RvD1 appears to mediate its effects via its receptors ALX/FPR2 and GPR32 [47]. In order to find which receptor is involved in the

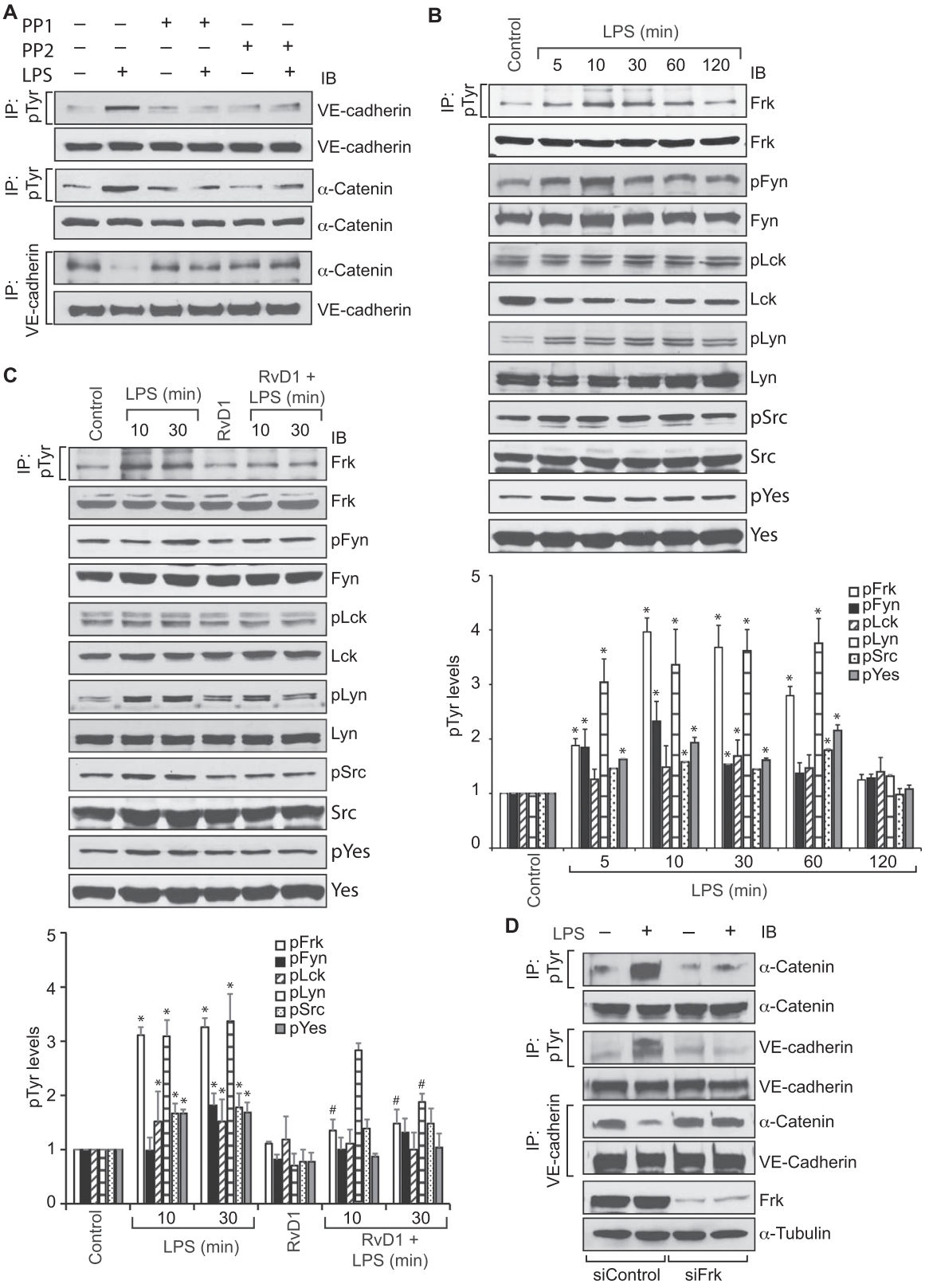

protective effects of RvD1 on endothelial AJ integrity and its barrier function, we tested their role using a pharmacological or neutralizing antibody approach. Western blot analysis showed that both ALX/FPR2 and GPR32 are expressed in HUVECs (Fig. 7A). Inhibition of ALX/FPR2 using its specific inhibitor, BOC2 [48], partially negated the effects of RvD1 in preventing LPS-induced XO activity, ROS produc-

Fig. 3. RvD1 inhibits Frk activation in blocking LPS-induced AJ protein Tyr phosphorylation and their disruption. A. Quiescent HUVECs were treated with and without LPS (500 ng/ml) in the presence and absence of PP1 (10 μM) or PP2 (10 μM), potent inhibitors of the Src family of tyrosine kinases, for 30 min and cell extracts were prepared. Equal amounts of proteins from control and each treatment were immunoprecipitated with pTyr or VE-cadherin antibodies and the immunocomplexes were analyzed by IB for the indicated proteins. B. Cell extracts of control and the indicated time periods of LPS (500 ng/ml)-treated HUVECs were either analyzed by WB for the indicated proteins or immunoprecipitated with pTyr antibodies and the immunocomplexes were immunoblotted for Frk. C. Quiescent HUVECs were treated with and without LPS (500 ng/ml) in the presence and absence of RvD1 (200 ng/ml) for the indicated time periods, cell extracts were prepared and analyzed for the phosphorylation of the indicated proteins as described in panel B. D. HUVECs that were transfected with siContol or siFrk and quiesced were treated with and without LPS (500 ng/ml) for 30 min, cell extracts were prepared and equal amounts of protein from control and each treatment were immunoprecipitated with pTyr or VE-Cadherin antibodies and the immunocomplexes were analyzed by IB for the indicated proteins. The same cell extracts were also analyzed by WB for Frk and α-Tubulin levels to show the effects of the siRNA on its target and off target molecules levels. E-G. All the conditions were the same as in panel D except that the quiescent HUVEC monolayer was treated with and without LPS (500 ng/ml) for 30 min, 2 h or the indicated time periods and stained for α-catenin and VE-cadherin as described in Figure legend 2E (E), subjected to dextran flux (F) and TER (G) assays, respectively. The bar graphs represent Mean ± SD values of three experiments. *, $p < 0.05$ vs control; #, $p < 0.05$ vs LPS.

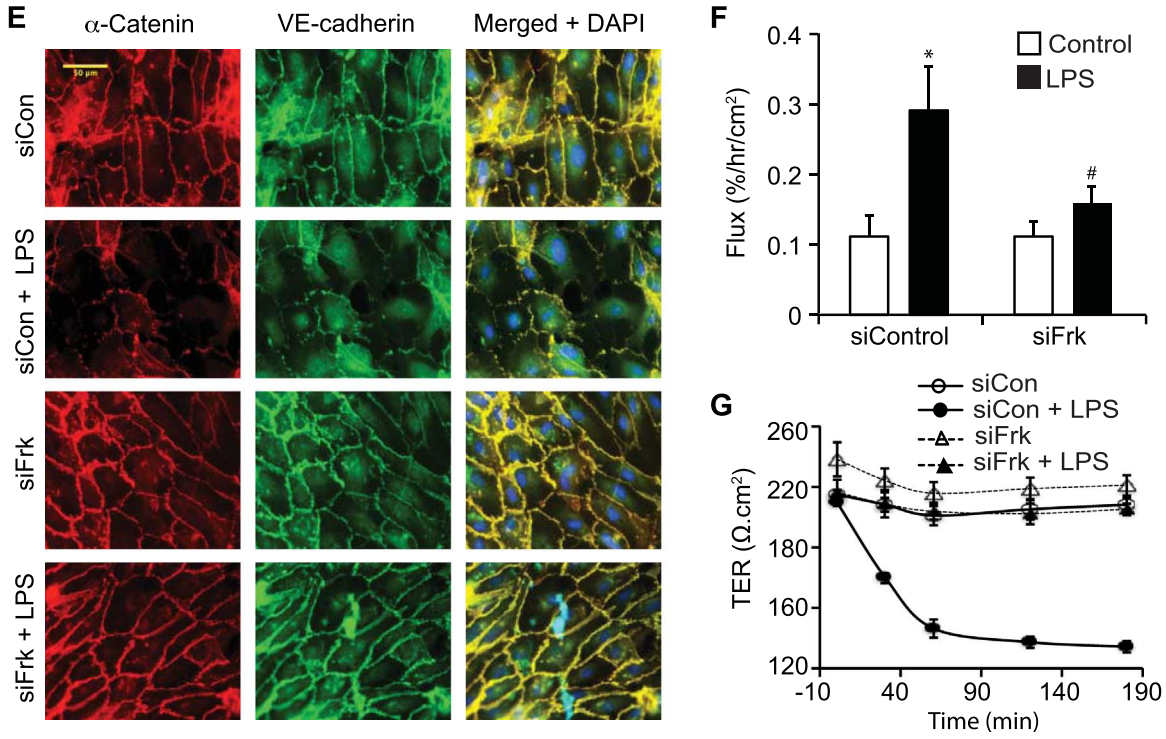

Fig. 3. (*continued*)

tion, SHP2 inhibition, Frk activation, α-catenin and VE-cadherin tyrosine phosphorylation and their dissociation from each other and from AJ and endothelial barrier permeability and reversing the decrease in its TER (Fig. 7B-G). Therefore, to understand whether RvD1 also acts through its other receptor GPR32, we have pretreated HUVECs with control IgG or GPR32 neutralizing antibodies (10 μg/ml) [49] alone or in combination with BOC2 and then tested the effect of RvD1 on LPS-induced endothelial AJ disruption and its barrier dysfunction. Neutralization of GPR32 alone exhibited almost the same level of inhibition as that of BOC2 on the effects of RvD1 in the reduction of LPS-induced XO activity, ROS production, SHP2 inhibition, Frk activation, α-catenin and VE-cadherin tyrosine phosphorylation and their dissociation from each other and from AJ, endothelial barrier permeability and decrease in its TER (Fig. 7H-N). However, when both the receptors were inhibited simultaneously, the preventive effects of RvD1 on LPS-induced XO activity, ROS production, SHP2 inactivation, Frk, α-catenin and VE-cadherin tyrosine phosphorylation, α-catenin and VE-cadherin dissociation from each other and from AJ, endothelial barrier permeability and decrease in its TER were completely lost (Fig. 7H-N).

3.6. RvD1 protects vascular AJ integrity and its permeability from LPS-induced disruption in vivo

To validate the protective effects of RvD1 on endothelial AJ integrity and its barrier function in vivo, mice that were administered first with RvD1 were challenged with LPS and 24 h later vascular permeability was measured by Miles assay or arteries were isolated and analyzed for either biochemical parameters or AJ integrity. LPS increased XO activity, SHP2 cysteine oxidation and its inactivation, Frk activation, α-catenin and VE-cadherin tyrosine phosphorylation and their dissociation from each other, AJ disruption and vascular permeability and RvD1 blocked all these effects in the arteries in vivo (Fig. 8A-G).

4. Discussion

Endothelial hyperpermeability is closely linked to various inflammatory vascular diseases such as atherosclerosis and thrombosis [19,21,22]. Endothelial cell-to-cell junctions play a critical role in the modulation of vascular permeability as well as its integrity [17,18]. Disruption in cell-to-cell contacts leads to increased vascular permeability and affects endothelial function [19]. Previously, it was reported that LPS increases endothelial barrier permeability by disrupting the TJ [11,12,50]. AJ and TJ are the important components of endothelial cell-to-cell adhesions and thus their barrier function [18,19]. It was proposed that AJ are also linked to the development of TJ [51]. Thus, disruption of not only TJ but also AJ could affect the overall vascular permeability and its integrity. Recent studies from many laboratories have shown that the endogenously derived metabolites of omega-3

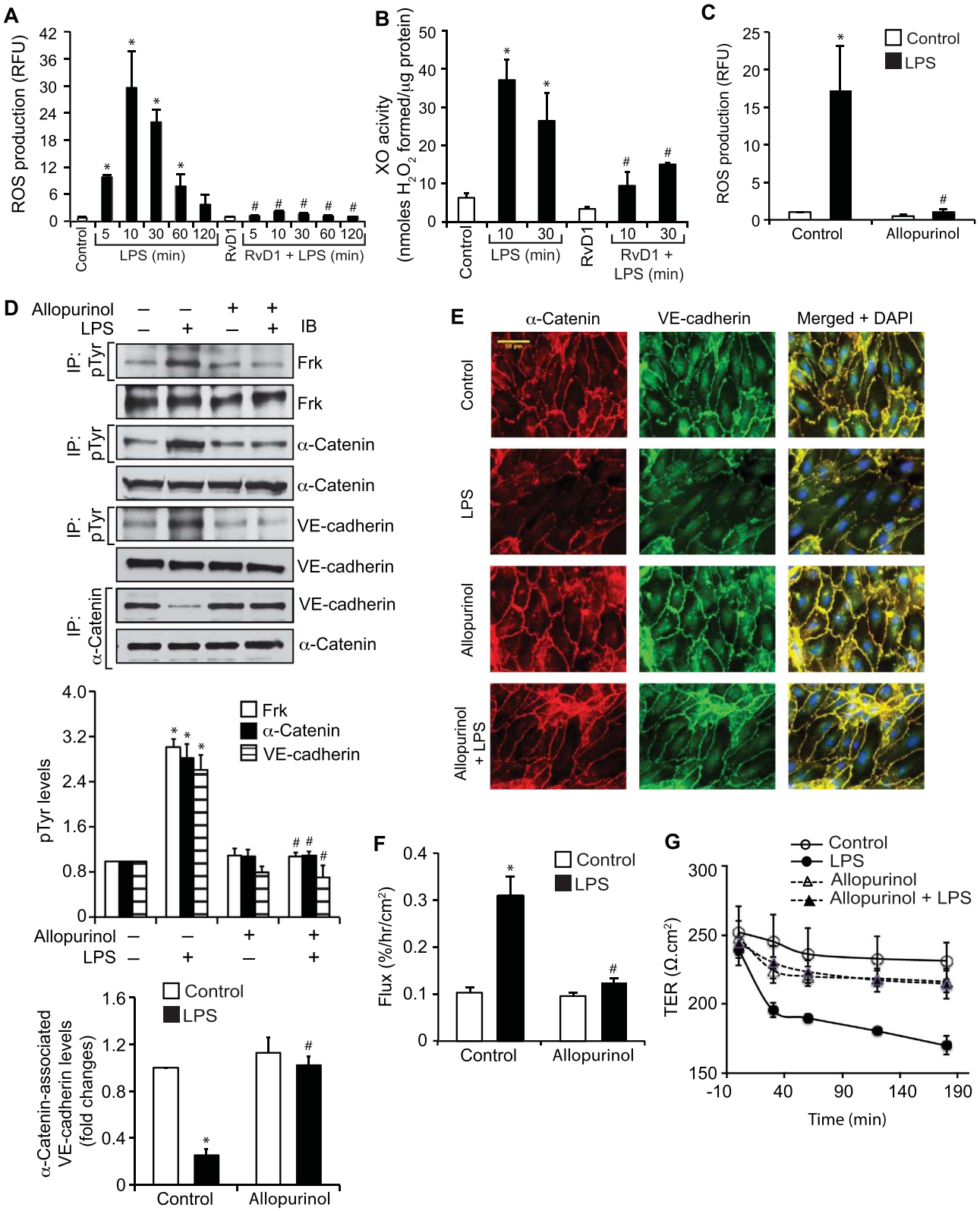

Fig. 4. RvD1 inhibits XO-mediated ROS production in blocking Frk activation and AJ disruption. A & B. Quiescent HUVECs were treated with and without LPS (500 ng/ml) in presence and absence of RvD1 (200 ng/ml) for the indicated time periods and ROS production (A) and XO activity (B) were measured. C. Quiescent HUVECs were treated with and without LPS (500 ng/ml) the presence and absence of Allopurinol (50 µM), XO inhibitor, for 30 min and ROS production was measured. D. All the conditions were same as in panel C except that an equal amount of protein from control and each treatment were immunoprecipitated with pTyr or α-catenin antibodies and the immunocomplexes were analyzed by IB for Frk, α-catenin and VE-cadherin using their specific antibodies. The same cell extracts was also analyzed by WB for their total levels. E-G. All the conditions were the same as in panel C except that the quiescent HUVEC monolayer after treatment with and without LPS (500 ng/ml) for 30 min, 2 h or the indicated time periods was stained for α-catenin and VE-cadherin as described in Figure legend 2E (E) or subjected to dextran flux (F) or TER (G) assays, respectively. The bar graphs represent Mean ± SD values of three experiments. *, $p < 0.05$ vs control; #, $p < 0.05$ vs LPS.

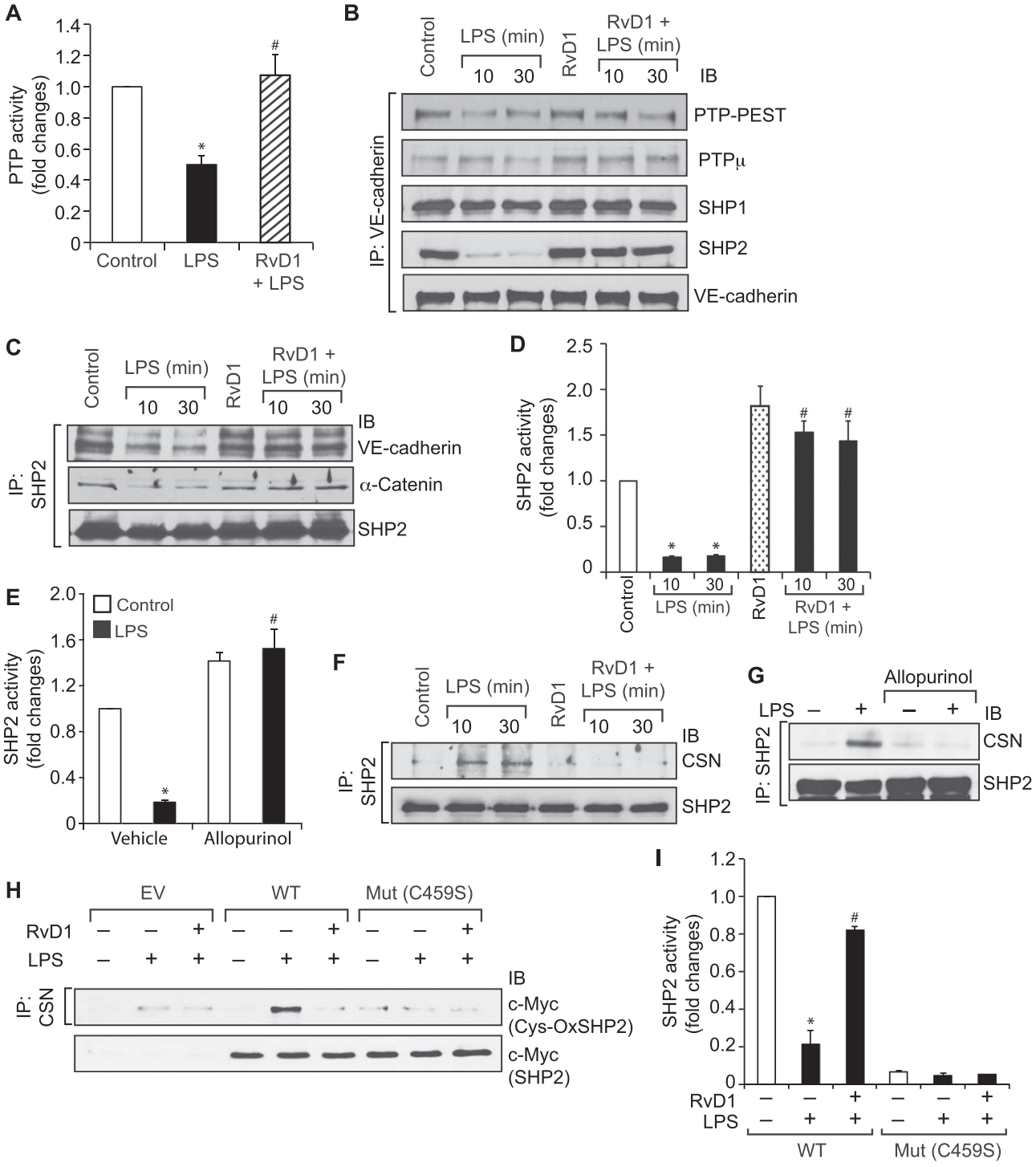

Fig. 5. RvD1 prevents LPS-induced SHP2 oxidation and its inactivation in the protection of AJ integrity. A. Quiescent HUVECs were treated with and without LPS (500 ng/ml) in presence and absence of RvD1 (200 ng/ml) for 30 min and PTP activity was measured using PTP-specific phosphopeptide as a substrate. B & C. Quiescent HUVECs were treated with and without LPS (500 ng/ml) in presence and absence of RvD1 (200 ng/ml) for the indicated time periods, cell extracts were prepared and equal amounts of protein from control and each treatment were immunoprecipitated with VE-cadherin or SHP2 antibodies and the immunocomplexes were analyzed by IB for the indicated proteins. D. All the conditions were same as in panel B except that after immunoprecipitation with SHP2 antibodies the immunocomplexes were assayed for SHP2 activity as described in panel A. E. Quiescent HUVECs that were treated with and without LPS (500 ng/ml) in the presence and absence of Allopurinol (50 μM) for 30 min were analyzed for SHP2 activity as described in panel D. F. All the conditions were same as in panel B except the cell extracts were immunoprecipitated with SHP2 antibodies and the immunocomplexes were immunoblotted for Cys sulphonate to measure SHP2 Cys oxidation and the blot was reprobed for total SHP2 levels. G. All the conditions were the same as in panel E except that the cell extracts were analyzed for SHP2 Cys oxidation as described in panel F and the blot was reprobed for total SHP2 levels. H. HUVECs were transiently transfected with empty vector (EV) or Myc-tagged recombinant SHP2 expression vector (WT and C459S mutant), grown to confluence, quiesced, treated with and without LPS (500 ng/ml) in the presence and absence of RvD1 (200 ng/ml) for 30 min and cell extracts were prepared. An equal amount of protein from control and each treatment was immunoprecipitated with Cysteine sulphonate antibody and the immunocomplexes were analyzed by IB for Myc to show SHP2 Cysteine oxidation. An equal amount of protein from control and each treatment was also analyzed by WB for Myc to show the overexpression of SHP2. I. HUVECs that were transfected with WT or mutant SHP2 expression vector and quiesced were treated with and without LPS (500 ng/ml) in the presence and absence of RvD1 (200 ng/ml) for 30 min and analyzed for SHP2 activity as described in panel D.

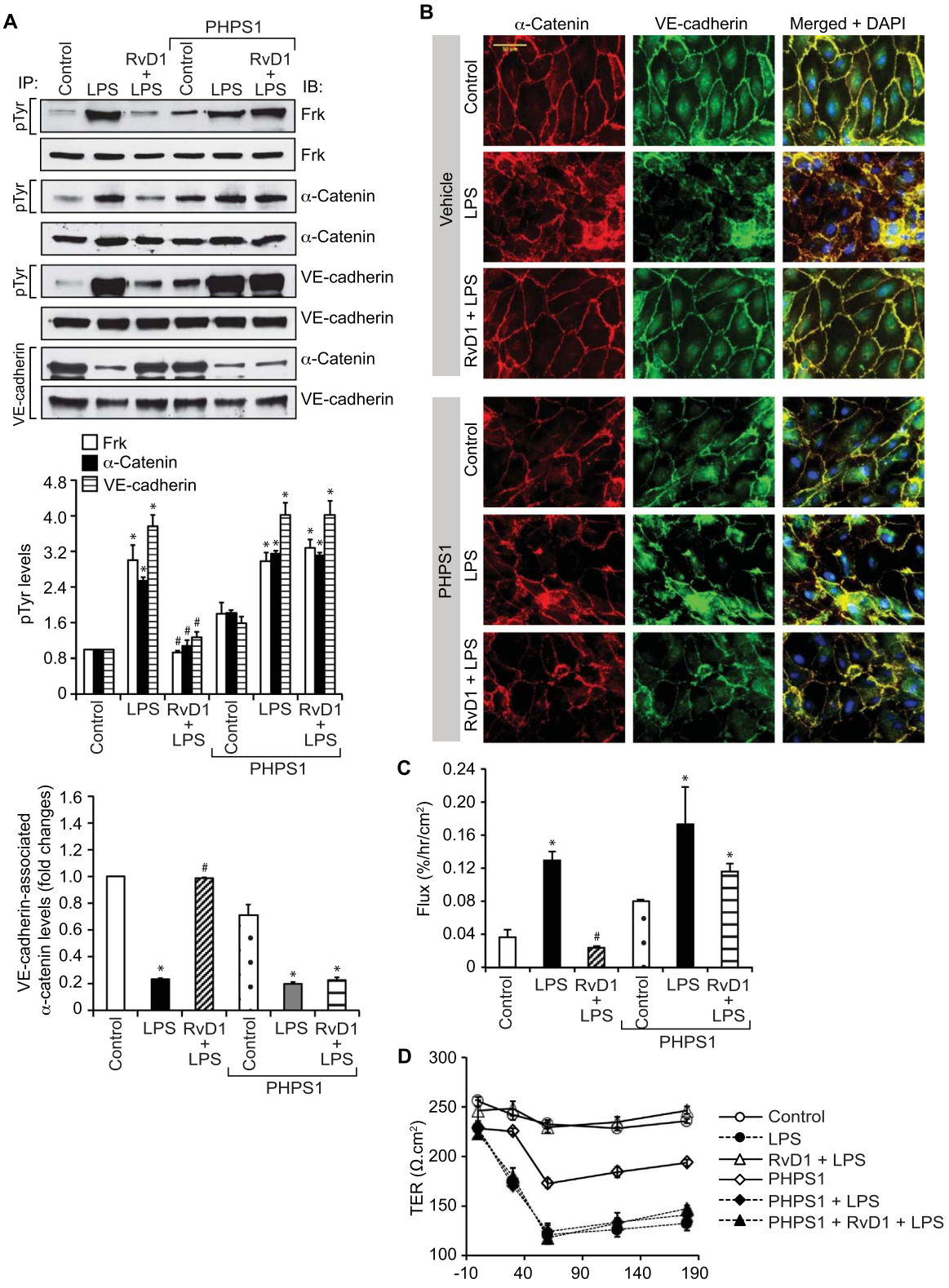

Fig. 6. Pharmacological inhibition of SHP2 blunts the capacity of RvD1 in the attenuation of LPS-induced Frk activation, α-catenin and VE-cadherin Tyr phosphorylation and AJ disruption. A. Quiescent HUVECs were treated with and without LPS (500 ng/ml) in the presence and absence of RvD1 (200 ng/ml) alone or in combination with or without PHPS1 (10 μM), a potent inhibitor of SHP2, for 30 min, cell extracts were prepared and an equal amount of protein from control and each treatment was immunoprecipitated with pTyr or VE-cadherin antibodies and the immunocomplexes were analyzed by IB for the indicated proteins. The same cell extracts were also analyzed for the indicated protein total levels. B. All the conditions were the same as in panel A except that the quiescent HUVEC monolayer after the treatments was stained double immunofluorescently for α-catenin and VE-cadherin as described in Figure legend 2E. C & D. Quiescent HUVEC monolayer was treated with and without LPS (500 ng/ml) in the presence and absence of RvD1 (200 ng/ml) alone or in combination with or without PHPS1 (10 μM) for 2 h or the indicated time periods and subjected to dextran flux (C) or TER (D) assays, respectively. The bar graphs represent Mean ± SD values of three experiments. *, $p < 0.05$ vs control; #, $p < 0.05$ vs LPS.

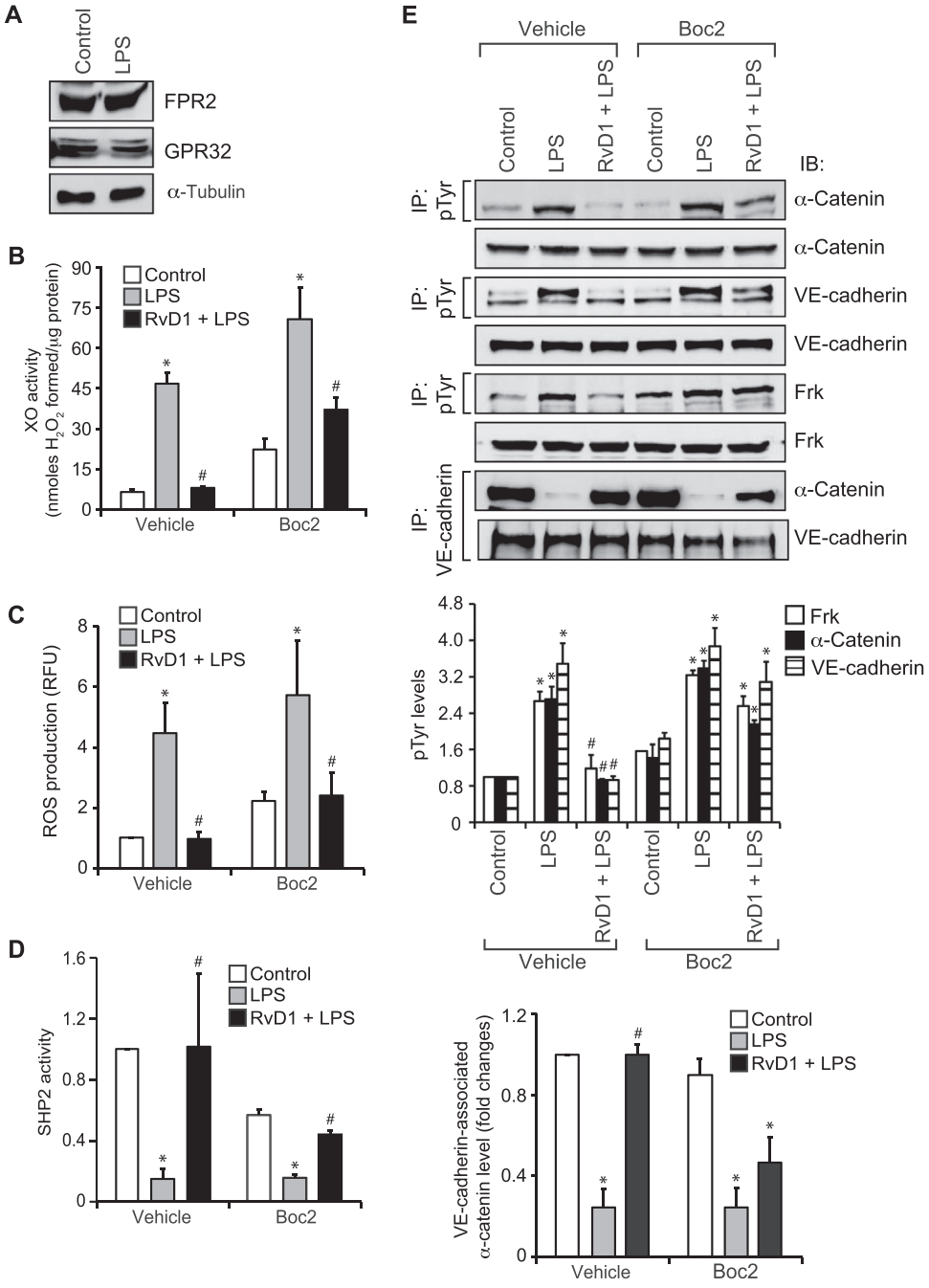

Fig. 7. Both ALX/FPR2 and GPR32 mediate the protective effects of RvD1 on LPS-induced endothelial AJ disruption and its barrier dysfunction. A. Cell extracts of control and various time periods of LPS (500 ng/ml)-treated HUVECs were analyzed by WB for ALX/FPR2 and GPR32 levels using their specific antibodies. B-D. Quiescent HUVECs were treated with and without LPS (500 ng/ml) in the presence and absence of RvD1 (200 ng/ml) in combination with and without Boc2 (3 μM), ALX/FPR2 inhibitor, for 30 min and XO activity (B), ROS production (C) and SHP2 activity (D) were measured. E. All the conditions were the same as in panel B except that cell extracts were prepared, and equal amounts of protein from control and each treatment were immunoprecipitated with pTyr or VE-Cadherin antibodies and the immunocomplexes were analyzed by IB for the indicated proteins using their specific antibodies. The same cell extracts were also analyzed by WB for the total levels of the indicated proteins. F & G. Quiescent HUVEC monolayer was treated with and without LPS (500 ng/ml) in the presence and absence of RvD1 (200 ng/ml) alone or in combination with and without Boc2 (3 μM) for 2 h or the indicated time periods and subjected to dextran flux (F) and TER (G) assays, respectively. H-J. Quiescent HUVECs were incubated with either control IgG or GPR32 IgG (10 μg/ml) alone or in combination with and without Boc2 (3 μM) for 30 min followed by treatment with and without LPS (500 ng/ml) in the presence and absence of RvD1 (200 ng/ml) for 30 min and XO activity (H), ROS production (I) and SHP2 activity (J) were measured. K. All the conditions were the same as in panel H except that cell extracts were prepared and equal amounts of protein from control and each treatment were immunoprecipitated with pTyr or VE-cadherin antibodies and the immunocomplexes were analyzed by IB for the indicated proteins using their specific antibodies. The same cell extracts were also analyzed by WB for the total levels of the indicated proteins. L. The quiescent HUVEC monolayer that was incubated with either control IgG, GPR32 IgG (10 μg/ml), Boc2 (3 μM) alone or in combination for 30 min followed by treatment with and without LPS (500 ng/ml) in the presence and absence of RvD1 (200 ng/ml) for 30 min was stained double immunofluorescently for α-catenin and VE-cadherin as described in Figure legend 2E. M & N. Quiescent HUVECs monolayer was incubated with either control IgG or GPR32 IgG (10 μg/ml) alone or in combination with and without Boc2 (3 μM) for 30 min followed by treatment with and without LPS (500 ng/ml) in the presence and absence of RvD1 (200 ng/ml) for 2 h or the indicated time periods and subjected to dextran flux (M) and TER (N) assays, respectively. The bar graphs represent Mean ± SD values of three experiments. *, $p < 0.05$ vs control or control IgG; #, $p < 0.05$ vs LPS or con IgG+LPS.

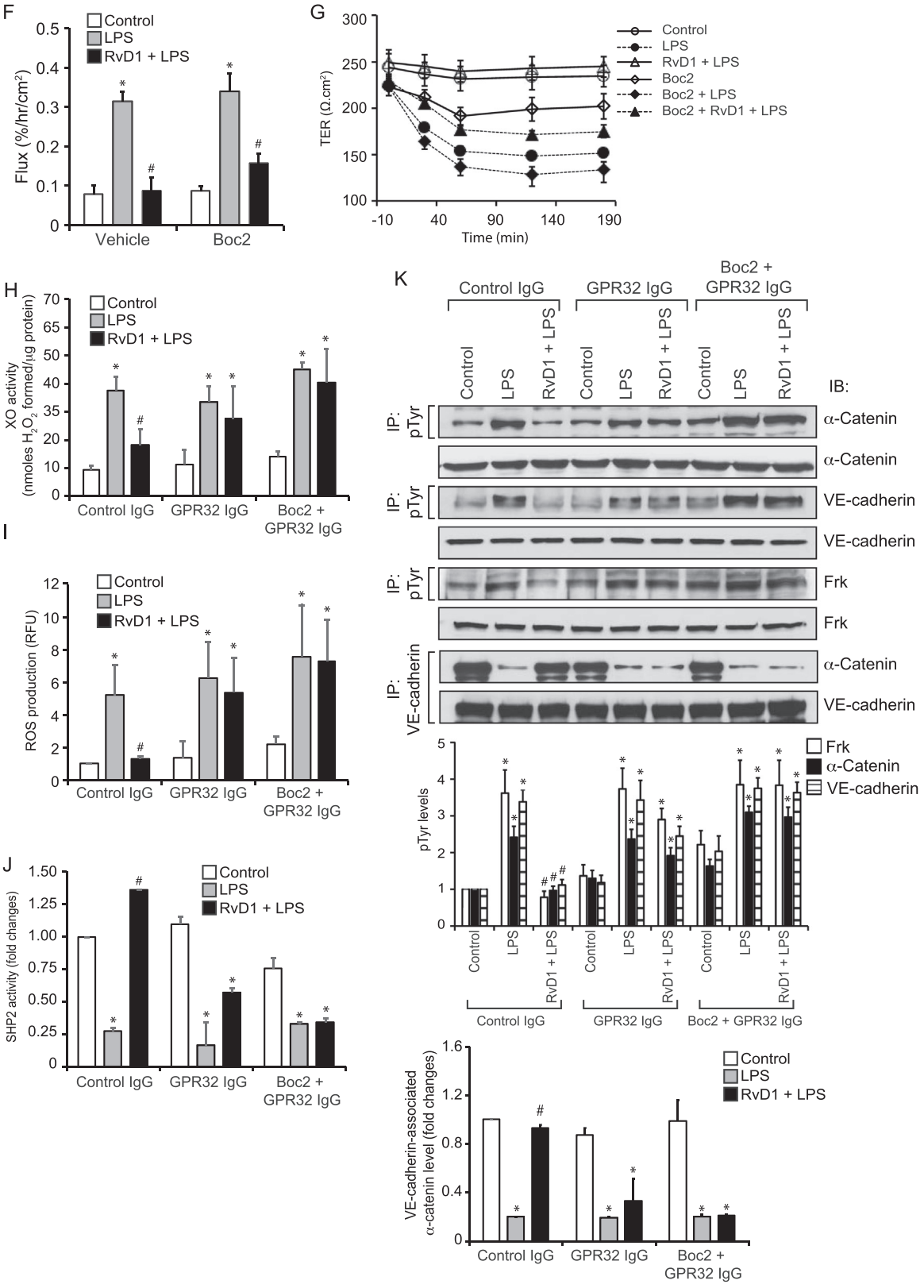

Fig. 7. (*continued*)

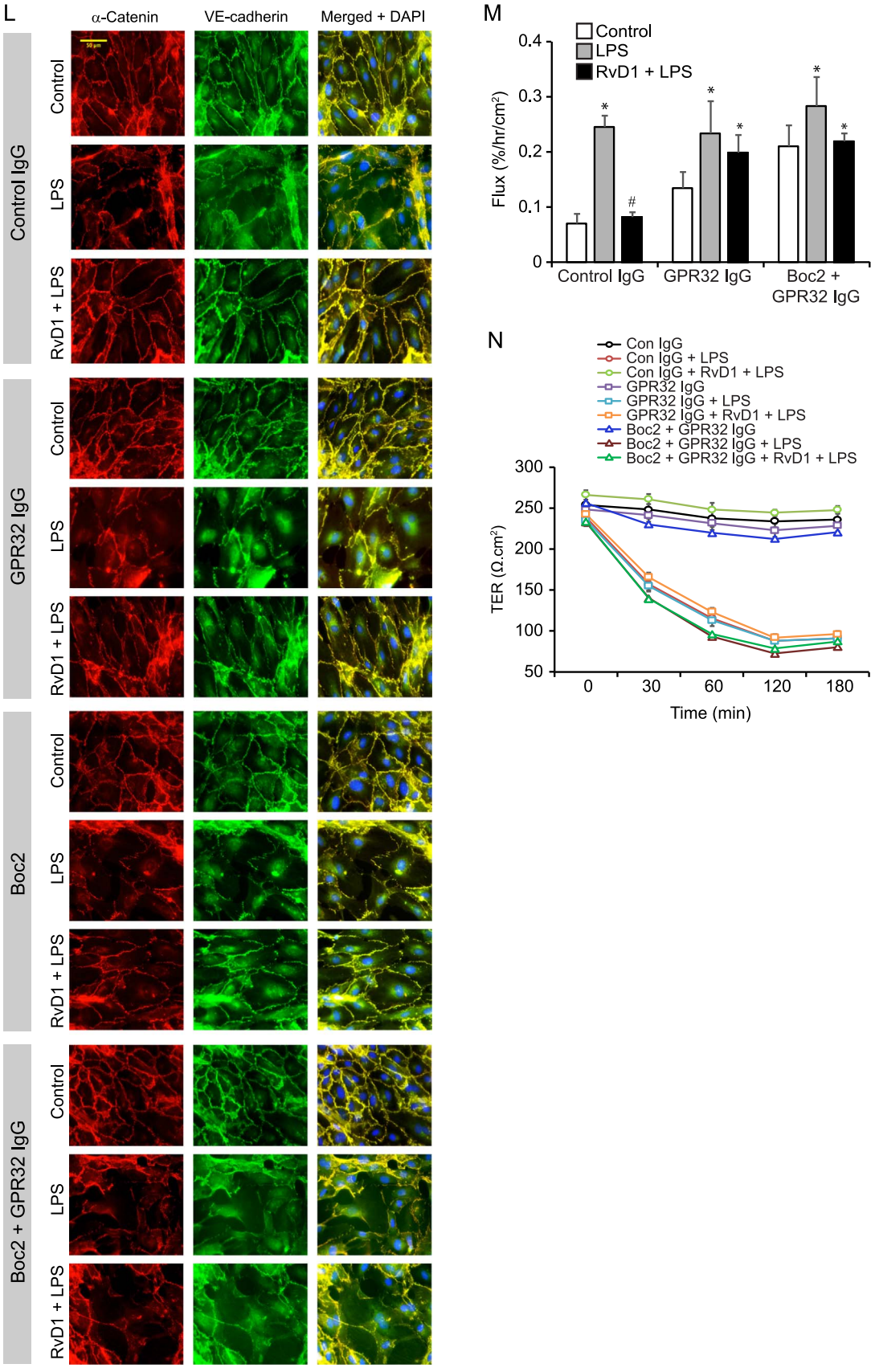

Fig. 7. (*continued*)

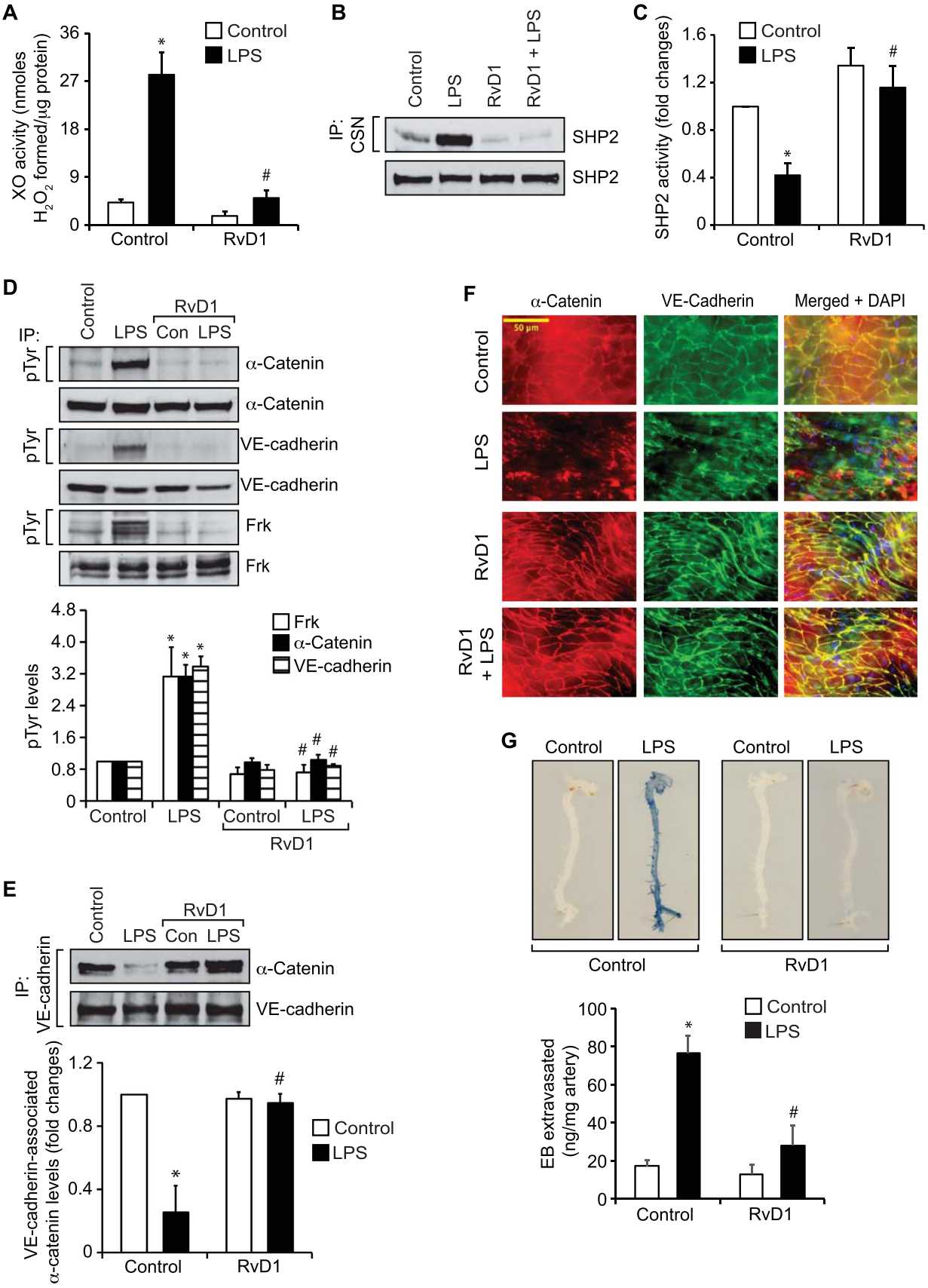
A
XO acivity (nmoles H_2O_2 formed/μg protein)
Control
LPS
Control
RvD1
B
Control
LPS
RvD1
RvD1 + LPS
IP: CSN
SHP2
SHP2
C
SHP2 activity (fold changes)
Control
LPS
Control
RvD1
D
IP:
Control
RvD1
LPS
Con
LPS
pTyr
α-Catenin
α-Catenin
pTyr
VE-cadherin
VE-cadherin
pTyr
Frk
Frk
pTyr levels
Frk
α-Catenin
VE-cadherin
Control
LPS
Control
LPS
RvD1
E
IP: VE-cadherin
Control
RvD1
LPS
Con
LPS
α-Catenin
VE-cadherin
VE-cadherin-associated α-catenin levels (fold changes)
Control
LPS
Control
RvD1
F
α-Catenin
VE-Cadherin
Merged + DAPI
50 μm
Control
LPS
RvD1
RvD1 + LPS
G
Control
LPS
Control
LPS
Control
RvD1
EB extravasated (ng/mg artery)
Control
LPS
Control
RvD1

Fig. 8. RvD1 attenuates LPS-induced aortic endothelial AJ disruption and hyper-permeability via blocking XO activity and SHP2 inactivation. A. C57BL/6 mice which were kept on chow diet were administered intraperitoneally with RvD1 (10 μg/kg body weight) every 2 days for 3 times before injecting LPS (5 mg/kg body weight) and 24 h later the aortas were isolated, tissue extracts were prepared and an equal amount of protein from each condition was analyzed for XO activity as described in Figure legend 4B. B. All the conditions were the same as in panel A except that tissue extracts containing an equal amount of protein from each condition were immunoprecipitated with Cys sulphonate antibodies and the immunocomplexes were analyzed by IB for SHP2. The same tissue extracts were analyzed by WB for total SHP2 levels. C. All the conditions were the same as in panel A except that tissue extracts were analyzed for SHP2 activity as described in Figure legend 5D. D & E. All the conditions were the same as in panel A except that tissue extracts were immunoprecipitated with pTyr (D) or VE-cadherin (E) antibodies and the immunocomplexes were analyzed by IB for the indicated proteins using their specific antibodies. The same tissue extracts were analyzed by WB for the indicated protein total levels. F. All the conditions were same as in panel A except that after isolation the aortas were opened longitudinally, fixed, permeabilized, blocked and co-immunostained for α-catenin and VE-cadherin as described in Figure legend 2E. G. All the conditions were the same as in panel A except that mice were anesthetized and 0.1 ml of 1% Evans Blue (EB) dye was injected into the tail vein. After 20 min, the blood vessels were perfused with PBS through the left ventriculum and the aortas were isolated and photographed. After taking the pictures, the aortas were minced, incubated in formaldehyde solution at 55 °C for 24 h, centrifuged and the optical density of the supernatant was measured at 610 nm in SpectraMax 190 spectrophotometer (Molecular Devices). The aortic endothelial barrier permeability was expressed as ng of EB dye extravasated per mg aorta. The bar graphs represent Mean ± SD values of three experiments with 2 animals/group or 5 animals minimum. *, $p < 0.05$ vs control; #, $p < 0.05$ vs LPS.

fatty acids, DHA and EPA, namely resolvin D and E series promote resolution of inflammation [5–7]. Some of these molecules have also been reported to exhibit atheroprotective effects [52–54]. Furthermore, it was found that the atherogenic conditions trigger a sustained depletion of their cellular levels [52], thus highlighting the importance of these lipid mediators in the resolution of inflammation and lesion regression. In this context, it was demonstrated that RvD1, the DHA metabolite, while enhancing anti-inflammatory cytokine expression inhibits neutrophil migration, reduces excessive PMN infiltration into the inflamed tissues, decreases PMN activation and ROS production, promotes phagocytosis and clearance of apoptotic cells as well as microbes and inhibits pro-inflammatory cytokine expression/secretion [5,9,10,55]. Supporting the role of these lipid mediators in the resolution of inflammation, it was further demonstrated that RvD1 protects endothelial TJ and its barrier function from LPS-induced disruption [11,12]. Although all these findings undoubtedly support the anti-inflammatory role of RvD1, the underlying mechanisms were not well understood. Towards exploring the underlying mechanisms of its anti-inflammatory functions, in this study we examined its effects on endothelial AJ integrity and its barrier function. Our findings show that RvD1 protects AJ from LPS-induced disruption. Specifically, RvD1 was found to block LPS-induced α-catenin and VE-cadherin tyrosine phosphorylation and their dissociation from each other as well as from AJ, thereby restoring AJ integrity and endothelial barrier function.

VE-Cadherin is a transmembrane component of AJ and exists in complex with a large number of intracellular molecules including α-catenin, β-catenin, γ-catenin and p120 catenin [13]. It also interacts with actin-binding proteins such as vinculin and eplin [13,18]. Its interaction with actin-binding proteins is critical for its role in the maintenance of the cytoskeleton and cell-to-cell junction stability [13,18]. More interestingly, VE-Cadherin interacts with actin-binding proteins via α-catenin [13]. In addition, many signaling molecules such as protein kinases and protein phosphatases have been found to be associated with VE-cadherin [19,25,27–29]. Thus, from its intricate protein-protein interacting architecture, it could be speculated that under different conditions VE-cadherin might form a complex with a specific protein either to increase or decrease the vascular permeability. Therefore, modulation of VE-cadherin expression or function could affect the overall stability of the endothelial cell-to-cell junctions and cytoskeleton. In fact, previous studies from other laboratories have suggested that phosphorylation-dependent VE-cadherin internalization and degradation leads to AJ disruption and increased endothelial barrier permeability [18,19,25,27,29]. In line with these observations, in the present study we found that LPS activates Frk in the phosphorylation of α-catenin and VE-cadherin leading to AJ disruption and endothelial barrier dysfunction. Cysteine residues at the active site of PTPs are usually negatively charged because of their low pKa values [56]. This negatively charged catalytic cysteine residues of the PTPs initiates the dephosphorylation of their substrates by nucleophilic attack at the phosphotyrosine phosphate group [57]. But this low pKa value also makes them more susceptible to oxidation by ROS [58]. In addition, it has been demonstrated that oxidation of PTP catalytic cysteine residues leads to their inactivation [45]. In this regard, the present findings reveal that LPS inactivates SHP2 via XO-mediated ROS production and oxidation of its catalytic cysteine residue, which in turn, leads to Frk activation, α-catenin and VE-cadherin tyrosine phosphorylation and their dissociation from each other disrupting endothelial AJ integrity and its barrier function. Furthermore, the findings that allopurinol, a potent inhibitor of XO, abolishes LPS-induced SHP2 cysteine oxidation and its inhibition, Frk activation, α-catenin and VE-cadherin tyrosine phosphorylation and their dissociation from each other promoting AJ integrity and endothelial barrier function support a role for XO-mediated SHP2 inhibition in LPS-induced AJ disruption and endothelial barrier dysfunction. As RvD1 is inhibiting XO activity and ROS production and preventing SHP2 catalytic cysteine oxidation and its inhibition resulting in the suppression of Frk activation and α-catenin and VE-cadherin tyrosine phosphorylation, it is likely that blocking SHP2 inhibition is the major mechanism of RvD1 in the protection of AJ and endothelial barrier function. This conclusion can be further supported by the observations that inhibition of SHP2 blocks the capacity of RvD1 to exert its protective effects in the attenuation of LPS-induced Frk activation, α-catenin and VE-cadherin tyrosine phosphorylation and their dissociation from each other as well as from AJ, AJ disruption and endothelial barrier dysfunction. RvD1 has been shown to exert its proresolving effects of inflammation via its receptors ALX/FPR2 and GPR32 [9,47,49]. In this context, our study further shows that inhibition of either receptor only partially negated the protective effects of RvD1 on AJ integrity and endothelial barrier function suggesting a role for the involvement of both the receptors in these effects. Indeed, when both the receptors were blocked, RvD1 completely lost its ability to prevent LPS-induced XO activity, ROS production, SHP2 inhibition, Frk activation, α-catenin and VE-cadherin tyrosine phosphorylation and their dissociation from each other as well as from AJ, AJ disruption and endothelial barrier dysfunction, which further reinforces the conclusion that both ALX/FPR2 and GPR32 are involved in the mediation of the protective effects of RvD1 against LPS-induced AJ disruption and endothelial barrier dysfunction. Furthermore, the present observations reveal that RvD1 inhibits LPS-induced XO activity, SHP2 cysteine oxidation and its inactivation, Frk activation, α-catenin and VE-cadherin tyrosine phosphorylation and their dissociation from each other, AJ disruption and vascular permeability in intact arteries in mice suggesting its protective effects on AJ integrity in vivo as well. However, further studies are required to identify the receptor(s) mediating the protective effects of RvD1 on AJ integrity in mice in vivo. It should be pointed out that RvD1 has also been reported to protect both epithelial and endothelial barrier integrity in a murine model of hydrochloric acid-induced acute lung injury [59]. This study has further demonstrated that RvD1 inhibits neutrophil and platelet interactions via reducing NFκB activation and proinflammatory cytokines such IL-1β and IL-6 expression. Based on these observations, it is possible that RvD1 could also negate LPS-induced NFκB activation and endothelial and monocyte/leukocyte interactions in attenuating inflammation, which remains to be explored. In addition, a recent study showed that the levels of specialized pro-resolving lipid mediators (SPM), including RvD1 were decreased in vulnerable regions of human

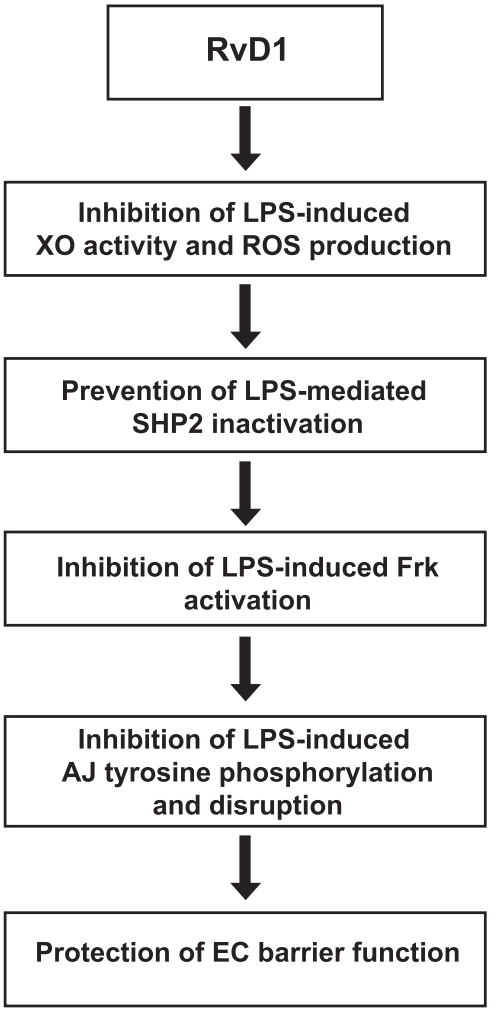

Fig. 9. Schematic diagram depicting the potential mechanism(s) by which RvD1 exerts its protective effects on endothelial AJ integrity and barrier function from LPS-induced disruption.

atherosclerotic plaques [60]. Furthermore, these authors showed that administration of RvD1 decreases oxidative stress and promotes plaque stability via resolution of inflammation. Based on all these observations, it is likely that SPM, including RvD1 may both inhibit inflammation and promote its resolution.

5. Conclusions

As summarized in Fig. 9, RvD1 via blocking LPS-induced XO activity and ROS production prevents SHP2 inactivation, and Frk activation and thereby inhibits Frk-mediated tyrosine phosphorylation of α-catenin and VE-cadherin and their dissociation from AJ in protecting EC barrier function from disruption by inflammatory molecules such as LPS.

Contributions

RC performed all the experiments and wrote the initial draft of the manuscript; SR performed Miles assay and Western blotting; GNR perceived the overall scope of the project, designed the experiments, interpreted the data and contributed in writing the manuscript.

Conflict of interest

None.

Acknowledgements

This work was supported by NIH grant HL074860 to GNR. The authors are thankful to Dr. Nikhlesh K. Singh for his assistance in tail vein injections.

References

[1] B.D. Levy, C.B. Clish, B. Schmidt, K. Gronert, C.N. Serhan, Lipid mediator class switching during acute inflammation: signals in resolution, Nat. Immunol. 2 (2001) 612–619.
[2] C.N. Serhan, J. Savill, Resolution of inflammation: the beginning programs the end, Nat. Immunol. 6 (2005) 1191–1197.
[3] J. Dalli, R.A. Colas, C.N. Serhan, Novel n-3 immunoresolvents: structures and actions, Sci. Rep. 3 (2013) 1940.
[4] R.E. Abdulnour, J. Dalli, J.K. Colby, N. Krishnamoorthy, J.Y. Timmons, S.H. Tan, R.A. Colas, N.A. Petasis, C.N. Serhan, B.D. Levy, Maresin 1 biosynthesis during platelet-neutrophil interactions is organ-protective, Proc. Natl. Acad. Sci. USA 111 (2014) 16526–16531.
[5] G.L. Bannenberg, N. Chiang, A. Ariel, M. Arita, E. Tjonahen, K.H. Gotlinger, S. Hong, C.N. Serhan, Molecular circuits of resolution: formation and actions of resolvins and protectins, J. Immunol. 174 (2005) 4345–4355.
[6] L.V. Norling, M. Spite, R. Yang, R.J. Flower, M. Perretti, C.N. Serhan, Cutting edge: humanized nano-proresolving medicines mimic inflammation-resolution and enhance wound healing, J. Immunol. 186 (2011) 5543–5547.
[7] C.N. Serhan, S. Hong, K. Gronert, S.P. Colgan, P.R. Devchand, G. Mirick, R.L. Moussignac, Resolvins: a family of bioactive products of omega-3 fatty acid transformation circuits initiated by aspirin treatment that counter proinflammation signals, J. Exp. Med. 196 (2002) 1025–1037.
[8] C.N. Serhan, N.A. Petasis, Resolvins and protectins in inflammation resolution, Chem. Rev. 111 (2011) 5922–5943.
[9] L.V. Norling, J. Dalli, R.J. Flower, C.N. Serhan, M. Perretti, Resolvin D1 limits polymorphonuclear leukocyte recruitment to inflammatory loci: receptor-dependent actions, Arterioscler. Thromb. Vasc. Biol. 32 (2012) 1970–1978.
[10] E. Titos, B. Rius, A. Gonzalez-Periz, C. Lopez-Vicario, E. Moran-Salvador, M. Martinez-Clemente, V. Arroyo, J. Claria, Resolvin D1 and its precursor docosahexaenoic acid promote resolution of adipose tissue inflammation by eliciting macrophage polarization toward an M2-like phenotype, J. Immunol. 187 (2011) 5408–5418.
[11] W. Xie, H. Wang, L. Wang, C. Yao, R. Yuan, Q. Wu, Resolvin D1 reduces deterioration of tight junction proteins by upregulating HO-1 in LPS-induced mice, Lab. Investig. 93 (2013) 991–1000.
[12] X. Zhang, T. Wang, P. Gui, C. Yao, W. Sun, L. Wang, H. Wang, W. Xie, S. Yao, Y. Lin, Q. Wu, Resolvin D1 reverts lipopolysaccharide-induced TJ proteins disruption and the increase of cellular permeability by regulating IkappaBalpha signaling in human vascular endothelial cells, Oxid. Med. Cell. Longev. 2013 (2013) 185715.
[13] G. Bazzoni, E. Dejana, Endothelial cell-to-cell junctions: molecular organization and role in vascular homeostasis, Physiol. Rev. 84 (2004) 869–901.
[14] D. Mehta, A.B. Malik, Signaling mechanisms regulating endothelial permeability, Physiol. Rev. 86 (2006) 279–367.
[15] J.S. Pober, W.C. Sessa, Evolving functions of endothelial cells in inflammation, Nat. Rev. Immunol. 7 (2007) 803–815.
[16] J.A. Vita, J.F. Keaney, Jr, Endothelial function: a barometer for cardiovascular risk?, Circulation 106 (2002) 640–642.
[17] E. Dejana, Endothelial cell-cell junctions: happy together, Nat. Rev. Mol. Cell. Biol. 5 (2004) 261–270.
[18] E. Dejana, C. Giampietro, Vascular endothelial-cadherin and vascular stability, Curr. Opin. Hematol. 19 (2012) 218–223.
[19] E. Dejana, E. Tournier-Lasserve, B.M. Weinstein, The control of vascular integrity by endothelial cell junctions: molecular basis and pathological implications, Dev. Cell 16 (2009) 209–221.
[20] I. Spadoni, E. Zagato, A. Bertocchi, R. Paolinelli, E. Hot, A. Di Sabatino, F. Caprioli, L. Bottiglieri, A. Oldani, G. Viale, G. Penna, E. Dejana, M. Rescigno, A gut-vascular barrier controls the systemic dissemination of bacteria, Science 350 (2015) 830–834.
[21] D.A. Chistiakov, A.N. Orekhov, Y.V. Bobryshev, Endothelial barrier and its abnormalities in cardiovascular disease, Front. Physiol. 6 (2015) 365.
[22] S.M. Weis, D.A. Cheresh, Pathophysiological consequences of VEGF-induced vascular permeability, Nature 437 (2005) 497–504.
[23] R.G. Oas, K. Xiao, S. Summers, K.B. Wittich, C.M. Chiasson, W.D. Martin, H.E. Grossniklaus, P.A. Vincent, A.B. Reynolds, A.P. Kowalczyk, p120-Catenin is required for mouse vascular development, Circ. Res. 106 (2010) 941–951.
[24] D. Nyqvist, C. Giampietro, E. Dejana, Deciphering the functional role of endothelial junctions by using in vivo models, EMBO Rep. 9 (2008) 742–747.
[25] E. Dejana, F. Orsenigo, M.G. Lampugnani, The role of adherens junctions and VE-cadherin in the control of vascular permeability, J. Cell Sci. 121 (2008) 2115–2122.
[26] P. Andriopoulou, P. Navarro, A. Zanetti, M.G. Lampugnani, E. Dejana, Histamine induces tyrosine phosphorylation of endothelial cell-to-cell adherens junctions, Arterioscler. Thromb. Vasc. Biol. 19 (1999) 2286–2297.
[27] S. Esser, M.G. Lampugnani, M. Corada, E. Dejana, W. Risau, Vascular endothelial growth factor induces VE-cadherin tyrosine phosphorylation in endothelial cells, J. Cell Sci. 111 (1998) 1853–1865.

[28] S. Baumer, L. Keller, A. Holtmann, R. Funke, B. August, A. Gamp, H. Wolburg, K. Wolburg-Buchholz, U. Deutsch, D. Vestweber, Vascular endothelial cell-specific phosphotyrosine phosphatase (VE-PTP) activity is required for blood vessel development, Blood 107 (2006) 4754–4762.
[29] S. Weis, S. Shintani, A. Weber, R. Kirchmair, M. Wood, A. Cravens, H. McSharry, A. Iwakura, Y.S. Yoon, N. Himes, D. Burstein, J. Doukas, R. Soll, D. Losordo, D. Cheresh, Src blockade stabilizes a Flk/cadherin complex, reducing edema and tissue injury following myocardial infarction, J. Clin. Invest. 113 (2004) 885–894.
[30] H.Y. Hsu, M.H. Wen, Lipopolysaccharide-mediated reactive oxygen species and signal transduction in the regulation of interleukin-1 gene expression, J. Biol. Chem. 277 (2002) 22131–22139.
[31] K.L. Grinnell, H. Chichger, J. Braza, H. Duong, E.O. Harrington, Protection against LPS-induced pulmonary edema through the attenuation of protein tyrosine phosphatase-1B oxidation, Am. J. Respir. Cell. Mol. Biol. 46 (2012) 623–632.
[32] S. Sukriti, M. Tauseef, P. Yazbeck, D. Mehta, Mechanisms regulating endothelial permeability, Pulm. Circ. 4 (2014) 535–551.
[33] R. Chattopadhyay, A. Tinnikov, E. Dyukova, N.K. Singh, S. Kotla, J.A. Mobley, G.N. Rao, 12/15-Lipoxygenase-dependent ROS production is required for diet-induced endothelial barrier dysfunction, J. Lipid Res. 56 (2015) 562–577.
[34] S. Kolli, C.I. Zito, M.H. Mossink, E.A. Wiemer, A.M. Bennett, The major vault protein is a novel substrate for the tyrosine phosphatase SHP-2 and scaffold protein in epidermal growth factor signaling, J. Biol. Chem. 279 (2004) 29374–29385.
[35] W. Xie, H. Wang, L. Wang, C. Yao, R. Yuan, Q. Wu, Resolvin D1 reduces deterioration of tight junction proteins by upregulating HO-1 in LPS-induced mice, Lab. Investig. 93 (2013) 991–1000.
[36] P. Wiesel, A.P. Patel, N. DiFonzo, P.B. Marria, C.U. Sim, A. Pellacani, K. Maemura, B.W. LeBlanc, K. Marino, C.M. Doerschuk, S.F. Yet, M.E. Lee, M.A. Perrella, Endotoxin-induced mortality is related to increased oxidative stress and end-organ dysfunction, not refractory hypotension, in heme oxygenase-1-deficient mice, Circulation 102 (2000) 3015–3022.
[37] A. Haziot, G.W. Rong, J. Silver, S.M. Goyert, Recombinant soluble CD14 mediates the activation of endothelial cells by lipopolysaccharide, J. Immunol. 151 (1993) 1500–1507.
[38] L. Li, J. Hu, T. He, Q. Zhang, X. Yang, X. Lan, D. Zhang, H. Mei, B. Chen, Y. Huang, P38/MAPK contributes to endothelial barrier dysfunction via MAP4 phosphorylation-dependent microtubule disassembly in inflammation-induced acute lung injury, Sci. Rep. 5 (2015) 8895.
[39] P.A. Ram, D.J. Waxman, Interaction of growth hormone-activated STATs with SH2-containing phosphotyrosine phosphatase SHP-1 and nuclear JAK2 tyrosine kinase, J. Biol. Chem. 272 (1997) 17694–17702.
[40] A.A. Miles, E.M. Miles, Vascular reactions to histamine, histamine-liberator and leukotaxine in the skin of guineapigs, J. Physiol. 118 (1952) 228–257.
[41] R. Chattopadhyay, E. Dyukova, N.K. Singh, M. Ohba, J.A. Mobley, G.N. Rao, Vascular endothelial tight junctions and barrier function are disrupted by 15(S)-hydroxyeicosatetraenoic acid partly via protein kinase C epsilon-mediated zona occludens-1 phosphorylation at threonine 770/772, J. Biol. Chem. 289 (2014) 3148–3163.
[42] A. Meneshian, G.B. Bulkley, The physiology of endothelial xanthine oxidase: from urate catabolism to reperfusion injury to inflammatory signal transduction, Microcirculation 9 (2002) 161–175.
[43] R. Butler, A.D. Morris, J.J. Belch, A. Hill, A.D. Struthers, Allopurinol normalizes endothelial dysfunction in type 2 diabetics with mild hypertension, Hypertension 35 (2000) 746–751.
[44] S. Guthikonda, C. Sinkey, T. Barenz, W.G. Haynes, Xanthine oxidase inhibition reverses endothelial dysfunction in heavy smokers, Circulation 107 (2003) 416–421.
[45] Z. Zhao, Z. Tan, J.H. Wright, C.D. Diltz, S.H. Shen, E.G. Krebs, E.H. Fischer, Altered expression of protein-tyrosine phosphatase 2C in 293 cells affects protein tyrosine phosphorylation and mitogen-activated protein kinase activation, J. Biol. Chem. 270 (1995) 11765–11769.
[46] K. Hellmuth, S. Grosskopf, C.T. Lum, M. Wurtele, N. Roder, J.P. von Kries, M. Rosario, J. Rademann, W. Birchmeier, Specific inhibitors of the protein tyrosine phosphatase Shp2 identified by high-throughput docking, Proc. Natl. Acad. Sci. USA 105 (2008) 7275–7280.
[47] S. Krishnamoorthy, A. Recchiuti, N. Chiang, S. Yacoubian, C.H. Lee, R. Yang, N.A. Petasis, C.N. Serhan, Resolvin D1 binds human phagocytes with evidence for proresolving receptors, Proc. Natl. Acad. Sci. USA 107 (2010) 1660–1665.
[48] A.L. Stenfeldt, J. Karlsson, C. Wenneras, J. Bylund, H. Fu, C. Dahlgren, Cyclosporin, H. Boc-MLF, and Boc-FLFLF are antagonists that preferentially inhibit activity triggered through the formyl peptide receptor, Inflammation 30 (2007) 224–229.
[49] H.M. Hsiao, T.H. Thatcher, E.P. Levy, R.A. Fulton, K.M. Owens, R.P. Phipps, P.J. Sime, Resolvin D1 attenuates polyinosinic-polycytidylic acid-induced inflammatory signaling in human airway epithelial cells via TAK1, J. Immunol. 193 (2014) 4980–4987.
[50] S. Guo, M. Nighot, R. Al-Sadi, T. Alhmoud, P. Nighot, T.Y. Ma, Lipopolysaccharide regulation of intestinal tight junction permeability is mediated by TLR4 signal transduction pathway activation of FAK and MyD88, J. Immunol. 195 (2015) 4999–5010.
[51] M. Itoh, A. Nagafuchi, S. Yonemura, T. Kitani-Yasuda, S. Tsukita, S. Tsukita, The 220-kD protein colocalizing with cadherins in non-epithelial cells is identical to ZO-1, a tight junction-associated protein in epithelial cells: cDNA cloning and immunoelectron microscopy, J. Cell Biol. 121 (1993) 491–502.
[52] J. Viola, P. Lemnitzer, Y. Jansen, G. Csaba, C. Winter, C. Neideck, C. Silvestre-Roig, G. Dittmar, Y. Doring, M. Drechsler, C. Weber, R. Zimmer, N. Cenac, O. Soehnlein, Resolving lipid mediators maresin 1 and resolvin D2 prevent atheroprogression in mice, Circ. Res. 119 (2016) 1030–1038.
[53] A.J. Merched, K. Ko, K.H. Gotlinger, C.N. Serhan, L. Chan, Atherosclerosis: evidence for impairment of resolution of vascular inflammation governed by specific lipid mediators, FASEB J. 22 (2008) 3595–3606.
[54] H. Hasturk, R. Abdallah, A. Kantarci, D. Nguyen, N. Giordano, J. Hamilton, T.E. Van Dyke, Resolvin E1 (RvE1) attenuates atherosclerotic plaque formation in diet and inflammation-induced atherogenesis, Arterioscler. Thromb. Vasc. Biol. 35 (2015) 1123–1133.
[55] K. Kasuga, R. Yang, T.F. Porter, N. Agrawal, N.A. Petasis, D. Irimia, M. Toner, C.N. Serhan, Rapid appearance of resolvin precursors in inflammatory exudates: novel mechanisms in resolution, J. Immunol. 181 (2008) 8677–8687.
[56] Z.Y. Zhang, J.E. Dixon, Active site labeling of the Yersinia protein tyrosine phosphatase: the determination of the pKa of the active site cysteine and the function of the conserved histidine 402, Biochemistry 32 (1993) 9340–9345.
[57] D. Barford, A.K. Das, M.P. Egloff, The structure and mechanism of protein phosphatases: insights into catalysis and regulation, Annu. Rev. Biophys. Biomol. Struct. 27 (1998) 133–164.
[58] A. Salmeen, D. Barford, Functions and mechanisms of redox regulation of cysteine-based phosphatases, Antioxid. Redox Signal. 7 (2005) 560–577.
[59] O. Eickmeier, H. Seki, O. Haworth, J.N. Hilberath, F. Gao, M. Uddin, R.H. Croze, T. Carlo, M.A. Pfeffer, B.D. Levy, Aspirin-triggered resolvin D1 reduces mucosal inflammation and promotes resolution in a murine model of acute lung injury, Mucosal Immunol. 6 (2013) 256–266.
[60] G. Fredman, J. Hellmann, J.D. Proto, G. Kuriakose, R.A. Colas, B. Dorweiler, E.S. Connolly, R. Solomon, D.M. Jones, E.J. Heyer, M. Spite, I. Tabas, An imbalance between specialized pro-resolving lipid mediators and pro-inflammatory leukotrienes promotes instability of atherosclerotic plaques, Nat. Commun. 7 (2016) 12859.